muscle possess the phosphoinositide-binding domain and are specifically targeted to the triads close to the DHPR–RYR1 complex. Cardiac isoforms do not contain this domain, suggesting that splicing of *BIN1* regulates its specific function in skeletal muscle. Immunofluorescence analyses of muscles from patients with *BIN1* mutations reveal aberrations of BIN1 localization and triad organization. These defects are also observed in X-linked and autosomal dominant forms of CNM and in *Mtm1* knockout mice. In addition to previously reported implications of BIN1 in cancer as a tumor suppressor, these findings sustain an important role for BIN1 skeletal muscle isoforms in membrane remodeling and organization of the excitation–contraction machinery. We propose that aberrant BIN1 localization and defects in triad structure are part of a common pathogenetic mechanism shared between the three forms of centronuclear myopathies.

Keywords Congenital myopathy · Centronuclear myopathy · Myotubular myopathy · Amphiphysin · Myotubularin · Dynamin · Triad · T-tubule

Abbreviations

ADCNM	Autosomal dominant centronuclear myopathy
ARCNM	Autosomal recessive centronuclear myopathy
BAR	Bin/Amphiphysin/Rvs167
CNM	Centronuclear myopathy
KO	Knockout
NADH-TR	Nicotinamide adenine dinucleotide tetrazolium reductase
OMIM	Online mendelian inheritance in man
PIs	Phosphoinositides
SR	Sarcoplasmic reticulum
XLMTM	X-linked myotubular myopathy

C. Wallgren-Pettersson
The Folkhälsan Institute of Genetics, 00290 Helsinki, Finland

V. Laugel
Service de Pédiatrie, Centre Hospitalier Universitaire (CHU) Hautepierre, 67091 Strasbourg, France

A. Echaniz-Laguna
Department of Neurology, Hôpital Civil, 67000 Strasbourg, France

I. Nishino
Department of Neuromuscular Research, National Institute of Neuroscience, National Center of Neurology and Psychiatry, Kodaira, Tokyo 187-8502, Japan

Introduction

Membrane remodeling is involved in diverse cellular functions, including endocytosis, intracellular transport, and synaptic vesicle recycling. BAR (Bin/Amphiphysin/Rvs167) adapter proteins are implicated in these processes through binding, curvature, and tubulation of membranes [16, 27, 38]. Recently, a member of the BAR proteins family, BIN1 (Bridging INtegrator-1), was found mutated in a rare form of congenital myopathy named centronuclear myopathy (CNM) [31], highlighting the implication of such proteins in neuromuscular diseases. However, the pathological mechanisms of *BIN1*-related CNM and possible common defects with other CNM forms are largely unknown.

BIN1 encodes for amphiphysin 2, a ubiquitous endocytic adaptor protein which was initially identified as a c-MYC-interacting pro-apoptotic tumor suppressor [41]. Reduction of *BIN1* expression in breast and other cancers was demonstrated, and introduction of *BIN1* into tumor cells lacking endogenous expression reduced their proliferative capacity [12, 29, 35, 41]. Several tissue-specific splice isoforms of *BIN1* have been described, e.g. a neuronal isoform implicated in synaptic vesicle endocytosis contains a clathrin and AP-2-binding domain, and a muscle isoform contains a polybasic residue sequence for binding to phosphoinositides (PIs), the PI-binding domain [21, 25, 36, 49]. Lee et al. [24] showed that this PI-binding domain was necessary for the membrane tubulation function of BIN1 in vitro and in cultured C2C12 myotubes. In skeletal muscle, BIN1 has been localized to T-tubules using a pan-isoform antibody [7]. T-tubules are plasma membrane invaginations that associate with the sarcoplasmic reticulum to form the triads, which are the functional units of the excitation–contraction coupling machinery [13]. Studies in Drosophila showed that mutation of the unique ortholog of mammalian amphiphysin 1 and BIN1 leads to disorganization of the T-tubule/sarcoplasmic reticulum (SR) system in body wall muscles, but did not impact on clathrin-mediated endocytosis [37]. Conversely, *Bin1* knockout mice did not have striking histological abnormalities in skeletal muscle, but resulted in perinatal cardiomyopathy, suggesting an important role of BIN1 in cardiac muscle development [28].

Congenital myopathies are a heterogeneous group of inherited neuromuscular disorders sharing muscle weakness and specific structural abnormalities in skeletal muscle fibers [32]. Among these diseases, centronuclear myopathies are characterized by prominent internalized or centralized nuclei in muscle fibers [18, 20, 30, 34]. CNMs have been divided into three forms: the severe X-linked form also called myotubular myopathy is due to mutations in the *MTM1* gene encoding the phosphoinositide phosphatase myotubularin (XLMTM, OMIM 310400) [23]; the autosomal dominant

form is due to mutations in *DNM2* coding for the large GTPase dynamin 2 implicated in membrane tubulation and fission (ADCNM, OMIM 160150) [3, 4]; the autosomal recessive form for which mutations in *BIN1* were recently reported in four families (ARCNM, OMIM 255200) [9, 31]. There was no specific cardiac or central nervous system involvement common to all these ARCNM patients. However, one of the reported patients had mild mental retardation [9]. Linkage analysis in spontaneous cases of CNM Labrador retrievers suffering from an autosomal recessive form of centronuclear myopathy led to the identification of a defective allele of the canine *PTPLA* gene, encoding a 3-hydroxyacyl-CoA dehydratase involved in very long-chain fatty acid synthesis [10, 33, 44]. Morpholino knockdown of myotubularin in Zebrafish resulted in abnormally located nuclei and muscle fiber hypotrophy with disorganized T-tubules structures and morphology [11]. Similar findings were reported in *Mtm1* knockout mouse muscles, where a generalized and progressive muscle weakness is detected from 3 to 4 weeks [1].

Until now, BIN1 has only been evaluated in a human pathological context related to cancer. While BIN1 appears to have a significant role in skeletal muscle, its specific function in this tissue is not well understood. Moreover, no molecular analyses of *BIN1*-mutated patients' muscles have been performed, and the link with the other forms of CNM has not been characterized. In this study, we investigate the expression and distribution of BIN1 in normal and diseased skeletal muscles from patients with confirmed mutations in *BIN1*, *MTM1*, or *DNM2* genes and from the existing mouse model for XLMTM. Our data establish for the first time a common pathogenetic mechanism for the three forms of CNM and point to a role for BIN1 in triad organization, specifically in skeletal muscle.

Materials and methods

Antibodies and materials

R2406 rabbit polyclonal antibody was generated for BIN1 against peptide RKKSKLFSRLRRKKN (corresponding to the PI-binding domain encoded by exon 11) as described [31]. Rabbit polyclonal antibodies against myotubularin were generated as described [45]. We used antibodies directed against the MYC-binding domain of BIN1 (C99D, Upstate), DHPR-alpha1 subunit (MA3-920, Affinity Bioreagents), RyR1 (clone 34C, Sigma), SERCA1 ATPase (MA3-911, ABR), alpha-actinin (EA-53, Sigma). *Mtm1* knockout mice were obtained by deletion of exon 4 as described [1, 6]. Care and manipulation of mice were performed in accordance with local, national, and European legislations on animal experimentation. Patients were enrolled on the basis of clinical and histopathological observations consistent with CNM, and genetic diagnosis was confirmed for all of them by direct sequencing of *MTM1*, *BIN1*, and *DNM2* coding sequences. We obtained informed consent from all patients or their families. Patients with MTM1 and the BIN1 Asp151Asn and Arg154Gln mutations were already reported [9, 22, 31, 47]. Detailed clinical analysis of the novel Gln573Stop mutation will be reported elsewhere. A summary is provided in Table 1.

RT-PCR

Total RNA was extracted from mouse spinal cord and skeletal and cardiac muscles using Trizol reagent (Tri reagent, MRCGENE) while human skeletal muscle RNA was purchased from Clontech. 1–2 μg of total RNA was used for reverse transcription to cDNA using Superscript II reverse transcriptase (Invitrogen) and random hexamers, according to manufacturers' instructions. The resulting cDNA was used for PCR amplification of full length BIN1, with the following primers: 5′ mouse BIN1, ATGGCAGAGATG GGGAGCAAGG; 3′ mouse BIN1, TCACTGCACCCGCT CTGTAAAATT; 5′ human BIN1, ACGGCGGGAAAGAT CGCCAG; 3′ human BIN1, TTGTGCTGGTTCCAGT CGCT. After PCR amplification, the resulting cDNAs were ligated into a PGEMTeasy vector (PROMEGA) and sequenced with ABI PRISM BigDye Terminator cycle using a 3130XL genetic analyzer (Applied Bioscience). The total number of isoforms identified and clones sequenced per tissue were: human skeletal muscle, three isoforms ($n = 31$ clones); mouse skeletal muscle, two isoforms ($n = 33$ clones); mouse cardiac muscle, three isoforms ($n = 30$ clones); and mouse spinal cord, five isoforms ($n = 34$ clones). Isoforms which represented more than 5% of total isoforms in one tissue are depicted in Fig. 3a.

Subcellular fractionation and protein expression analyses

For subcellular fractionation, microsomal (S) and cytoskeleton (P) fractions were prepared from freshly dissected *tibialis anterior* muscles from wild-type and *Mtm1* KO mice as described [39]. For protein expression analysis in human biopsies, tissues were crushed by ultra turax in TGEK50 buffer (50 mM Tris pH 7.8, 10% glycerol, 1 mM EDTA, 50 mM KCl) with 0.1% SDS, 2% Triton X-100, 10 mM sodium vanadate, 1 mM beta-glycerophosphate, 1 mM NaF, and the protease inhibitors cocktail. For western blotting, incubation with primary antibodies was performed for 1 h (1:5,000 anti-BIN1 R2406 polyclonal antibody) at RT or overnight at 4°C. Secondary antibodies (anti-rabbit-Horseradish Peroxidase or anti-mouse-HRP, Jackson ImmunoResearch) were incubated for 1 h at RT.

Table 1 Patients with centronuclear myopathies analyzed in this study

Gene	Age (years)	Muscle	Mutation	CNM	Clinical course
MTM1	1	Biceps brachii	p.Asp380 frameshift	XLMTM	Severe infantile form. Marked muscle weakness and hypotonia with respiratory insufficiency since birth
MTM1	1	Biceps brachii	p.Ser420_Arg421 insertionFIQ	XLMTM	Severe infantile form. Marked muscle weakness and hypotonia with respiratory insufficiency since birth
BIN1	27, 36	Deltoid	p.Asp151Asn	ARCNM	Onset at 8 years, stable
BIN1	19	Deltoid	p.Arg154Gln	ARCNM	Diffuse muscle atrophy from 11 years, very slow progression of the disease
BIN1	12	Quadriceps	p.Gln573Stop	ARCNM	Onset at 5.5 years, stable
DNM2	16	Gastrocnemius	p.Glu368Lys	ADCNM	Childhood onset. Died when 16 years old due to pneumonia associated with respiratory insufficiency
DNM2	37	Biceps brachii	p.Arg465Trp	ADCNM	Onset at 10 years, stable

The most common mutations in MTM1 and DNM2 are p.Ser420_Arg421 insertionFIQ and p.Arg465Trp, respectively

Mutation nomenclature is based on *MTM1* (human *MTM1*, Genbank U46024), *BIN1* (human *BIN1*, Genbank NM_139343), and *DNM2* (human *DNM2*, Genbank NM_001005360) cDNA sequences

XLMTM X-linked myotubular (centronuclear) myopathy (OMIM 310400), *ARCNM* autosomal recessive centronuclear myopathy (OMIM 255200), *ADCNM* autosomal dominant centronuclear myopathy (OMIM 160150)

Histological analyses

For CNM patients, the number of muscle biopsies, the name of muscles, and the age of patients when the muscle biopsies were performed are indicated in Table 1. For controls, we used biopsies from seven different individuals [5 days (newborn), 1.5 months, 4 months, 14 months, 14 years, 31 years, and 46 years old]. Control muscles used for morphological analysis (4 months, 14 years, and 46 years old) were quadriceps. 10 μm transverse sections from CNM patients' frozen biopsies were stained with hematoxylin–eosin, NADH-TR, and ATPase using standard protocols [8, 26]. The percentage of centralized, internalized and peripheral nuclei, and percentages of type I and II fibers were calculated in consecutive non-overlapping 100× high-powered fields (hpf). Nuclei were counted as "internalized" when they were neither in the center (centralized) nor adjacent to the sarcolemma (peripheral).

Immunofluorescence

Mice were anesthetized by intraperitoneal injection of 5 μl/body gram of ketamine (20 mg/ml, Virbac) and xylazine (0.4%, Rompun, Bayer) and perfused with 4% paraformaldehyde prior to muscle dissection. The dissected quadriceps muscles were then post-fixed in the same fixative for 2 h and cryo-protected overnight in PBS containing 2.3 M sucrose. Human and murine muscle biopsies were frozen in liquid nitrogen-cooled isopentane. 10 μm sections were incubated for 1 h at RT with primary antibodies against BIN1 anti-PI domain, DHPR-alpha, RYR1, SERCA1, or alpha-actinin, then 45 min with secondary antibodies (Alexa fluor 488 goat anti-rabbit antibody, Alexa fluor 555 or 594 goat anti-mouse antibodies, Invitrogen). Fluorescence was examined with a Leica SP2-AOBS confocal microscope. Pictures were processed with Tcstk and Dvrtk softwares (Jean-Luc Vonesch, Imaging Center, IGBMC) and Photoshop 7.0 (Adobe).

Ultrathin sections and electron microscopy

Biopsies were fixed with 4% paraformaldehyde, 0.1% glutaraldehyde in 0.1 M phosphate buffer, cryoprotected with 2.3 M sucrose and frozen in liquid nitrogen. For resin embedding, the frozen samples were substituted in methanol containing 2% osmium tetroxide, 0.25% uranyl acetate, and 0.25% glutaraldehyde, rinsed with pure methanol, with acetone, infiltrated with graded concentrations of epon (30, 50, 70, and 100%), and the resin was polymerized at 60°C for 2 days. Ultrathin sections were obtained on a Leica Ultracut S ultramicrotome. Staining was performed with uranyl acetate and lead citrate. Image acquisition was done with a Philips CM12 electron microscope operated at 80 kV and equipped with an Orius 1000 CCD camera (GATAN).

Results

Common morphological abnormalities in centronuclear myopathies

Muscle histopathology in ARCNM patients mutated in *BIN1* was not compared to date as only data on two patients

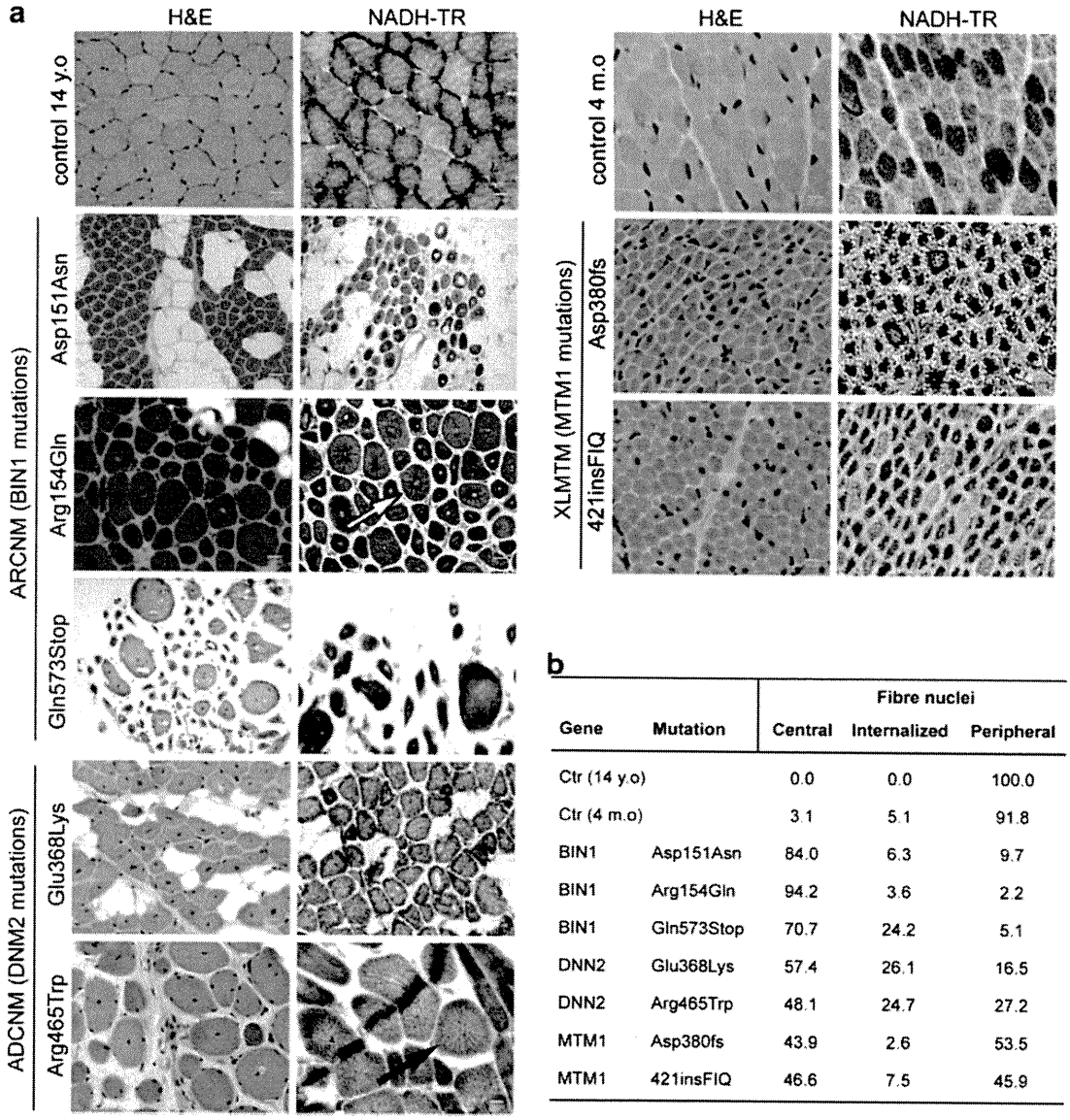

b

Gene	Mutation	Fibre nuclei		
		Central	Internalized	Peripheral
Ctr (14 y.o)		0.0	0.0	100.0
Ctr (4 m.o)		3.1	5.1	91.8
BIN1	Asp151Asn	84.0	6.3	9.7
BIN1	Arg154Gln	94.2	3.6	2.2
BIN1	Gln573Stop	70.7	24.2	5.1
DNN2	Glu368Lys	57.4	26.1	16.5
DNN2	Arg465Trp	48.1	24.7	27.2
MTM1	Asp380fs	43.9	2.6	53.5
MTM1	421insFIQ	46.6	7.5	45.9

Fig. 1 Comparison of the muscle histopathology in patients with different CNM forms. **a** Cross-sections of muscle biopsies from CNM patients with MTM1, BIN1, or DNM2 mutations compared with controls (4 months and 14 years old), stained with hematoxylin and eosin (H&E, *left panels*) or with nicotinamide adenine dinucleotide tetrazolium reductase activity (NADH-TR, *right panels*). While internalization of nuclei and variations in fiber size are common features of centronuclear myopathies, radial organization of sarcoplasmic strands is found in biopsies from patients with DNM2 mutations (*arrow*) and in some fibers from patients with BIN1 mutations (*arrow*), but not in patients with MTM1 mutations. Fat cell/connective tissue infiltrates were more prominent in the BIN1-mutated biopsies. *Scale bar* 20 μm. **b** Quantification of the central, internalized, and peripheral nuclei as a percentage of total nuclei, using H&E staining. Nuclei were counted as "internalized" where they were neither in the center nor adjacent to the sarcolemma. There was a higher percentage of centralized nuclei in all three BIN1-related biopsies; a high percentage of internalized nuclei was not linked to a specific CNM form

were independently reported [9, 31]. In order to characterize further their histopathological phenotype and compare with other CNM forms, we collected biopsies from patients with XLMTM, ARCNM, and ADCNM (Table 1). All CNM biopsies showed variation in myofiber size and a strong increase in nuclei centralization ranging from 43 to 94%, with the three *BIN1*-related biopsies showing the highest number of centralization (Fig. 1). Type 1 fiber predominance was observed in all CNM biopsies, ranging from 61 to 75% (Table 2; Supplementary Fig. 1), in the upper limit or above normal range when compared to normal values found in the same muscles [19]. Concerning *BIN1*-related biopsies, we noted a predominant accumulation of fat cell infiltrates. NADH-TR-stained

Table 2 Percentage of type I and type II fibers observed in CNM patients

Gene	Mutation	Muscle	Type I (%)	Type II (%)
BIN1	p.Asp151Asn	Deltoid	61	39
DNM2	p.Glu368Lys	Gastrocnemius	64	36
DNM2	p.Arg465Trp	Biceps brachii	68	32
MTM1	p.Ser420_Arg421 insertionFIQ	Biceps brachii	75	25

Normal distribution of fiber types is based on the work of Johnson and colleagues [19] and is as follows (mean percentage of type I, observed range in six male subjects): deltoid (57, range 43–67), gastrocnemius (48, range 35–60), biceps brachii (46, range 37–61)

biopsies displayed a differential aggregation of oxidative activity in *BIN1*-related biopsies, with an abnormal concentration around the central nuclei and beneath the sarcolemma (Fig. 1). We found that some fibers from *BIN1*-related biopsies showed a radial organization of sarcoplasmic strands, previously thought to be characteristic for *DNM2*-mutated muscles and used as a differential diagnostic feature between ADCNM and XLMTM. However, the radiating strands appeared less frequent in *BIN1*-related biopsies than in *DNM2*-related biopsies. Clusters of centralized nuclei were seen only in *BIN1*-related biopsies, and this specificity might be used to prioritize the genetic diagnosis toward *BIN1* sequencing. There were no obvious "necklace" fibers found in late-onset XLMTM [2]. Altogether, these results showed that biopsies from patients with three distinct *BIN1* mutations displayed histopathological hallmarks shared with other CNM forms.

Ultrastructural defects in CNM muscles with BIN1 mutations

We used electron microscopy to further address the phenotypic changes of *BIN1*-mutated muscles. Besides the typical features of CNM, like mitochondria and glycogen accumulation around the central nuclei (Fig. 2a, b), both patients analyzed presented additional abnormalities not previously emphasized in the different forms of CNM. In the Asp151Asn biopsy, accumulation of vacuoles containing degradation products under the sarcolemma and the presence of internalized and externalized vesicles-like structures suggested abnormal process of autophagy and exocytosis (Fig. 2c). Moreover, we noted sarcolemmal invaginations with accompanying basement membrane converging toward the central part of fibers (Fig. 2e, g). For the Gln573Stop mutation in the SH3 domain, we observed accumulation of mitochondria and caveolae beneath the sarcolemma (Fig. 2d). The latter appeared implicated in invaginations into the myofibers (Fig. 2f). We also observed slight defects in triad morphology, which included enlarged T-tubules associated with SR cisternae or normal-sized T-tubules surrounded by enlarged SR cisternae (Fig. 2h). Altogether, these data support ultrastructural alterations in *BIN1*-related ARCNM, most probably linked to membrane remodeling at the plasma membrane region and at the triad. Identification of additional *BIN1*-mutated patients will be required to confirm this correlation.

BIN1 skeletal muscle-specific isoforms are targeted to the triad

BIN1 encodes at least ten different RNA isoforms [36, 49]. Isoform 8 contains the PI-binding domain encoded by exon 11 and is highly expressed in skeletal muscle [24, 31]. As mutations in *BIN1* lead to congenital myopathy affecting primarily skeletal muscle without recurrent cardiac involvement, we further characterized BIN1 isoforms by RT-PCR followed by cDNA cloning (Fig. 3a). The two main isoforms in skeletal muscle both encompassed exon 11 and differed by the inclusion or exclusion of exon 17. Isoform 1, which contains the clathrin-binding domain, was not present in muscles and spinal cord suggesting that the BIN1 protein is not bound to clathrin in these tissues. Skeletal and cardiac muscles clearly differed by the presence or absence of exon 11, respectively.

We characterized BIN1 subcellular expression pattern during myofiber growth using the R2406 antibody directed against the PI-binding domain encoded by exon 11. In human muscles, BIN1 localization switched from longitudinal (newborn) to transverse orientation (3.4 months and adult) during the final muscle maturation (Fig. 3b). A previous study using a pan-isoform antibody showed that BIN1 was present on T-tubules in skeletal muscle [7]. Using our isoform-specific antibody we observed that BIN1 localized on structures corresponding to the triads as it colocalized with the T-tubule marker DHPR-alpha and with the ryanodine receptor RYR1 in skeletal muscles from 2- and 5-week-old mice (Fig. 4a, c). We confirmed that the BIN1 PI-binding domain was absent in cardiac muscle (Fig. 4e). Altogether, these data suggest that BIN1 is associated with triads before their transverse reorganization during skeletal muscle development and specifically contains the PI-binding domain encoded by exon 11 in this tissue. We used this *BIN1* domain-specific antibody in subsequent experiments.

BIN1 and triad abnormalities in myotubularin-deficient mice

A well-characterized mammalian model for X-linked myotubular myopathy is the *Mtm1* KO mouse that appears asymptomatic during the first few weeks and develops a

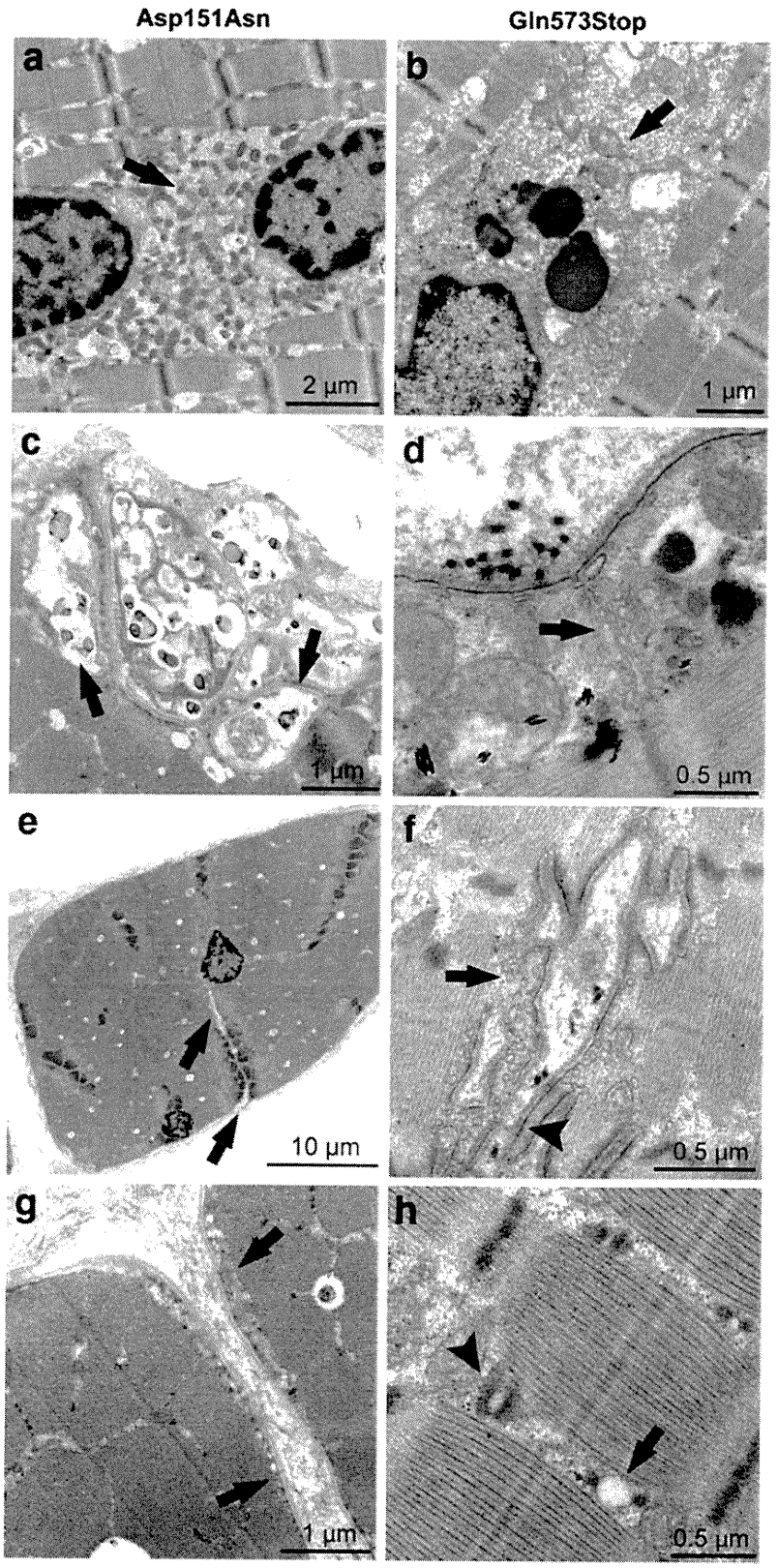

Fig. 2 Ultrastructural defects in ARCNM with confirmed *BIN1* mutations. Electron microscopy analysis of deltoid and quadriceps muscle biopsies from two ARCNM patients with an Asp151Asn missense mutation in the membrane tubulating N-BAR domain (**a**, **c**, **e**, **g**) or a Gln573Stop mutation truncating the SH3 C-terminal domain (**b**, **d**, **f**, **h**). Both biopsies displayed disorganization of muscle fibers with central nuclei surrounded by mitochondria and glycogen as seen in other forms of CNM (*arrows* in **a**, **b**). In addition, the Asp151Asn biopsy showed numerous vacuoles under the sarcolemma, which contained apparent degradation products and frequently showed a basal lamina demonstrating the sarcolemmal nature (**c**, *arrows*). The Asp151Asn biopsy also showed sarcolemma invagination pointing to the center of fibers (**e**, **g**, *arrows*). **g** is an enlargement of an invagination in direction of the fiber center (at the *bottom* of the image). The Gln573Stop biopsy displayed accumulation of caveolea (**d**, **f**, *arrows*), membrane invaginations (**f**, *arrowhead*), and defects in triad morphology as enlarged T-tubules (**h**, *arrow*) or enlarged sarcoplasmic reticulum cisternae (**h**, *arrowhead*)

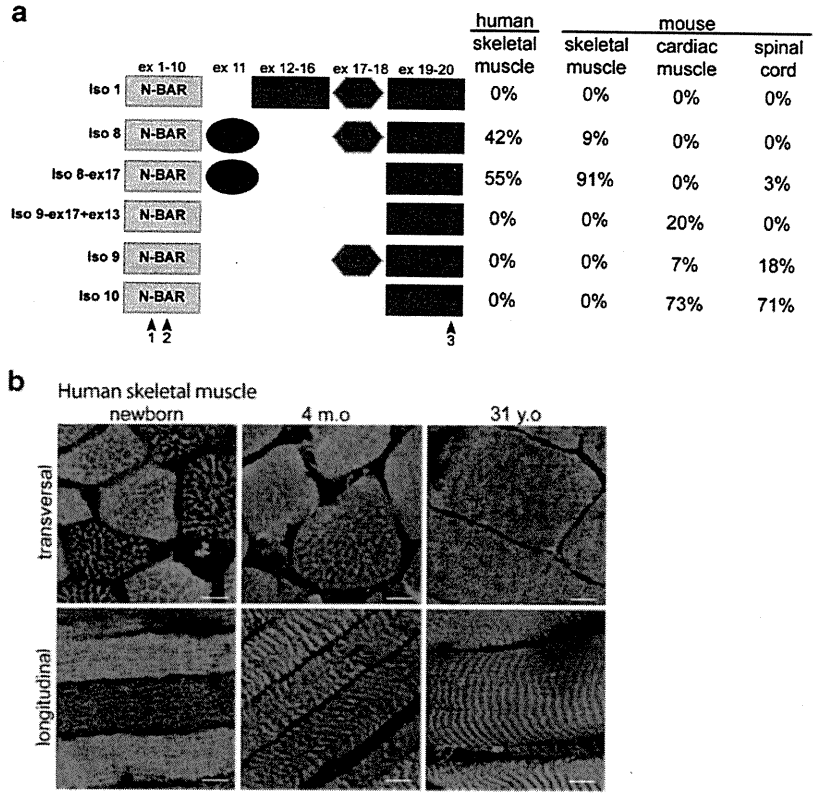

Fig. 3 BIN1 isoforms in wild-type skeletal and cardiac muscles. **a** Schematic representation of BIN1 protein domains, corresponding exons, and isoforms. Mutations corresponding to the patients' biopsies used in this study are indicated with *arrowheads*: *1* Asp151Asn, *2* Arg154Gln, *3* Gln573Stop. *N-BAR* N-terminal amphipathic helix and Bin-Amphiphysin-Rvs domain that induce and maintain membrane curvature, *PI* phosphoinositides-binding domain, *CBD* clathrin-binding domain, *MBD* MYC-binding domain, *SH3* Src Homology domain mediating protein–protein interactions. Isoforms representation was determined by RT-PCR followed by cDNA cloning and sequencing. Percentages of clones corresponding to the different isoforms are indicated for the different tissues (n = 22–34 clones per tissue). Minor cDNAs found only once are not shown. Iso1 is the main isoform known in brain, and we discovered two novel isoforms lacking exon 17 that encodes part of the MBD. Exon 13 encodes part of the CBD; exon 11 encodes the PI-binding domain. **b** Distribution of the PI-binding domain of BIN1 (R2406 antibody) in human skeletal muscle of newborn, 3.4-month- and 31-year-old controls. *Scale bar* 10 μm

progressive muscle weakness from 3 weeks of age [6]. Compared to the typical striated pattern of triads in wild-type skeletal muscle, BIN1 presented abnormalities in localization, e.g. regions lacking BIN1 labeling and irregular deviation from the transverse orientation, in 2-week-old mice which do not have detectable muscle weakness (Fig. 4a, b; arrowheads). Such defects were also observed in 5-week-old *Mtm1*-deficient muscles (Fig. 2c, d; arrowheads and enlargements), an age when mice display muscle weakness and a histological phenotype similar to XLMTM patients. Different planes of the muscle sections showed similar findings. In parallel, we confirmed a similar disorganization of DHPR and RYR1 labeling, while alpha-actinin and SERCA1 were not predominantly altered (Fig. 4b, d; Supplementary Fig. 2) [1]. In addition, BIN1 was not significantly released from membranes in *Mtm1* KO muscles as the BIN1 ratio between sarcolemmal and cytoplasmic/cytoskeletal proteins was not shifted toward the cytosol (Fig. 4g). Altogether, these observations suggest that BIN1 mislocalization is linked to defects of the underlying membrane structure and precedes the appearance of muscle weakness in *Mtm1*-deficient muscles.

Skeletal muscle-specific isoforms of *BIN1* were not expressed in cardiac muscles from 5-week-old wild-type or *Mtm1*-deficient mice, which displayed a normal striated signal of the T-tubule marker, DHPR-alpha (Fig. 4e, f). These results correlate well with the absence of major heart involvement in *Mtm1* KO mice and in XLMTM patients mutated in *MTM1*, and with the specific expression of BIN1 PI-binding domain in skeletal muscle.

Abnormal BIN1 localization in several forms of centronuclear myopathies

We assessed the distribution of BIN1 by immunofluorescence in biopsies from neonatal XLMTM (*MTM1*) cases,

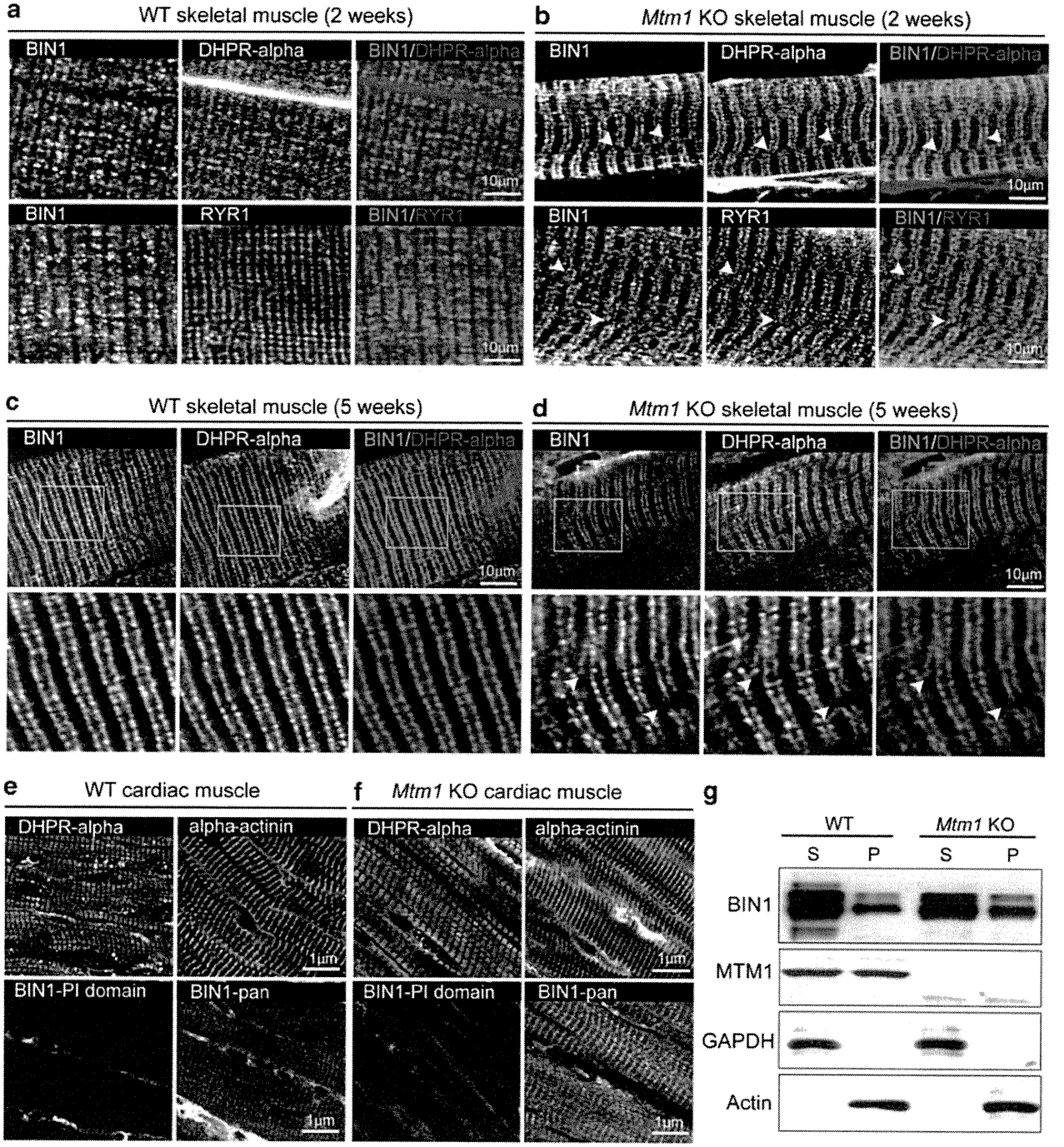

Fig. 4 BIN1 and T-tubule disorganization in a mouse model of X-linked myotubular myopathy. BIN1 PI-binding domain was detected with the specific R2406 antibody, T-tubule with anti-DHPR-alpha and sarcoplasmic reticulum with anti-RYR1 (triad) on longitudinal 10 μm sections from **a** skeletal muscles from 2-week-old wild-type (WT) and **b** *Mtm1* KO mice, **c** skeletal muscles from 5-week-old wild-type (WT) and **d** *Mtm1* KO mice. 2-week-old *Mtm1* KO mice are pre-symptomatic, while 5-week-old mice display muscle weakness and muscle fiber hypotrophy. *Arrowheads* point to abnormal orientation of BIN1, RYR1, and DHPR-alpha staining. **e**, **f** BIN1 was detected with the R2406 antibody against the PI-binding domain or with the R2444 antibody that recognizes all isoforms, T-tubule with anti-DHPR-alpha and the Z-line with anti-alpha-actinin, on longitudinal sections from **e** cardiac muscles from 5-week-old wild-type (WT) and **f** *Mtm1* KO mice. Note that the PI domain of BIN1 is not detectable in cardiac muscle fibers. BIN1 labeling appears *green* on the merge pictures. Different planes of the muscle sections were analyzed. Confocal pictures: *scale bar* **a**–**d** 10 μm, **e**, **f** 1 μm. **g** Subcellular fractionation of skeletal muscles from WT and *Mtm1* KO mice probed with antibodies against the BIN1 PI-binding domain, MTM1, GAPDH, and actin. *S* supernatant (corresponding to the microsomal fraction), *P* pellet

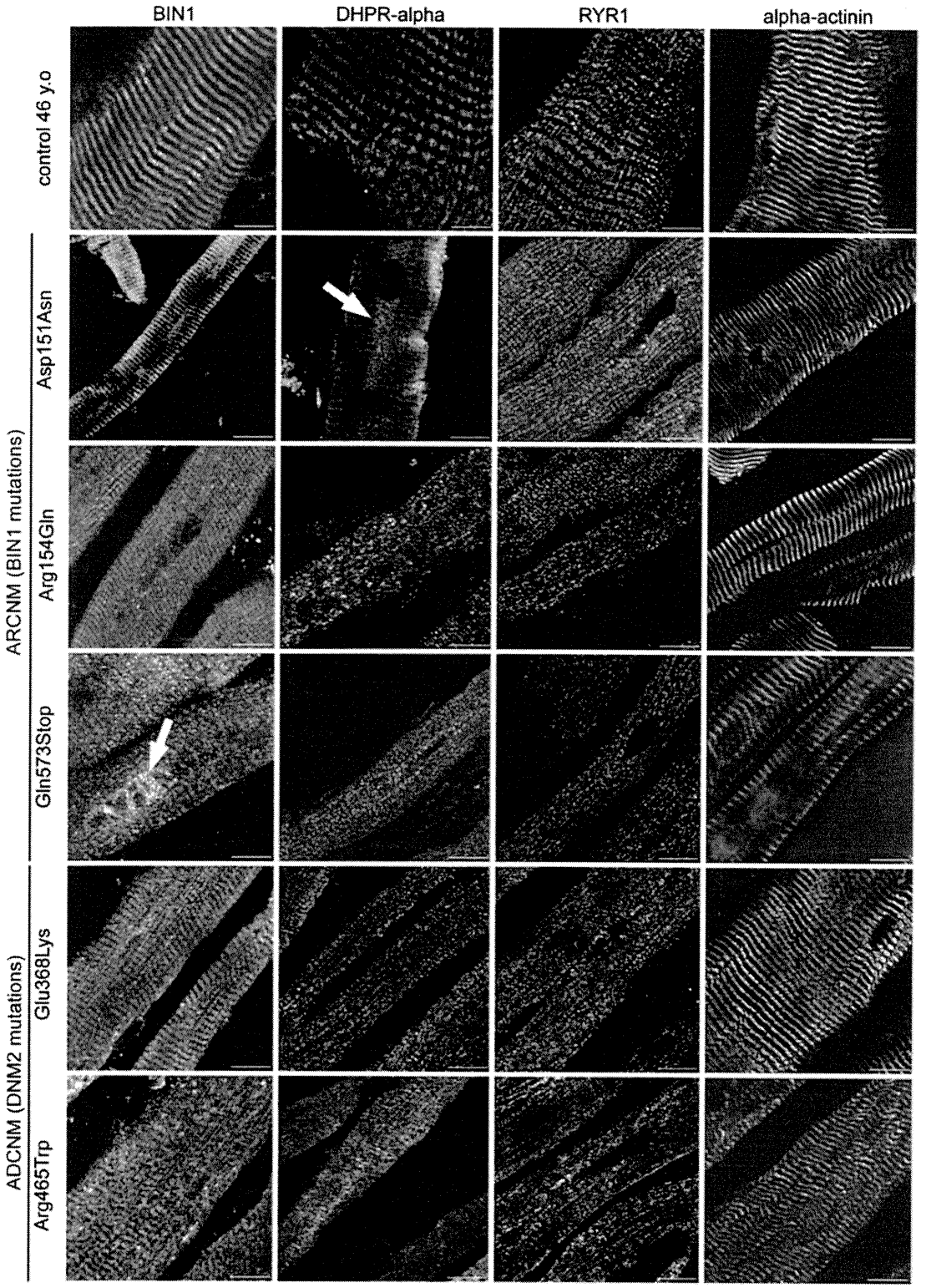

or ARCNM (*BIN1*) and ADCNM (*DNM2*) adolescent/adult cases using neonatal (1.5 months old) or adult (46 years old) skeletal muscles as controls, respectively. In all CNM cases, we observed defects of BIN1 localization, albeit with variability between the different forms (Figs. 5, 6). The most striking defect was for the most common DNM2

◀ **Fig. 5** BIN1 and T-tubule/triad defects in ARCNM and ADCNM forms of centronuclear myopathies. Immunolocalization of BIN1, DHPR-alpha, RYR1, and alpha-actinin in muscle biopsies from patients with mutations in *DNM2* or *BIN1*, as indicated, compared to control (46 years old). BIN1 is detected but mislocalized around central nuclei (*arrows*) or in longitudinal orientation in *BIN1*-mutated muscles and was similarly affected in other forms of CNM. Z-line organization appeared normal, while defect in triad markers organization ranged from abnormal orientation of the striated structures to accumulation (*arrows*) of these markers. Different planes of the muscle sections were analyzed. Confocal pictures: *scale bar* 10 μm

mutation, Arg465Trp, associated with the classical mild adult-onset form, where the distribution of BIN1 appeared in a longitudinal orientation in different planes of the sections instead of the transverse orientation typically observed in wild-type adult skeletal muscle (Fig. 5). This suggests possible accumulation of BIN1 mislocalization with time in *DNM2*-related patients. In all CNM samples, BIN1 transverse localization was less prominent than in controls (Fig. 5). In addition, we also observed some accumulations of BIN1 in the center of fibers, often around central nuclei, in biopsies with *BIN1* and *MTM1* mutations (Figs. 5, 6; arrows). We conclude that BIN1 mislocalization is common to several forms of CNM. ARCNM is not due to an absence of BIN1 protein, but rather to decreased association with triads and/or to structural defects of the triads. In agreement, BIN1 level appeared normal in patient fibroblasts by western blot analysis [31]. Follow-up was available for patient ADR71 (Asp151Asn BIN1 mutation) from 10 to 36 years of age with muscle biopsies taken at 27 and 36 years; he showed a very slow progression of muscle weakness and no visible differences in BIN1 labeling and histology between the two biopsies (not shown).

Structural defects of the triads are common to several forms of centronuclear myopathies

From neonate to adult muscles, the T-tubule (DHPR-alpha) and triad (RYR1) markers reorganized from a longitudinal to a transverse localization (Figs. 5, 6) in a spatio-temporal pattern mimicking that of BIN1 (Fig. 3). This result confirmed that terminal maturation of triads occurs soon after birth in humans [15]. All CNM patients' biopsies showed defects of these markers ranging from abnormal orientation of the striated structures in all CNM cases to accumulation in the center of fibers in the patient with Asp151Asn BIN1 mutation (Fig. 5; arrow). *BIN1*-related biopsies showed an abnormal longitudinal positioning of triads. In *MTM1*-related biopsies, even if markers of the triads were in a longitudinal orientation like in control neonatal muscles, we observed an abnormal accumulation of RYR1 in discrete areas of the fibers (Fig. 6; arrows). The most striking abnormalities for triad proteins expression were observed

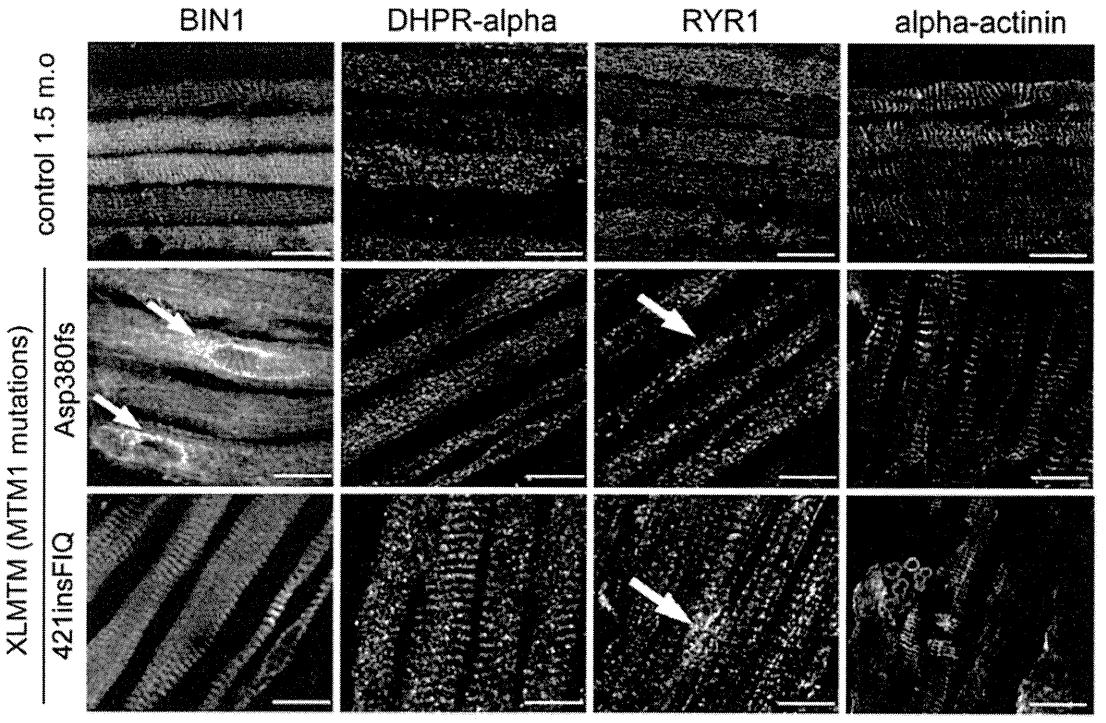

Fig. 6 BIN1 and T-tubule/triad defects in XLMTM. Immunolocalization of BIN1, DHPR-alpha, RYR1, and alpha-actinin in muscle biopsies from patients with mutations in *MTM1* compared to control (1.5 months old). BIN1 is detected but mislocalized around central nuclei (*arrows*) in *MTM1*-mutated muscles. Z-line organization appeared normal, while triad markers organization was abnormal with some accumulations (*arrows*). Different planes of the muscle sections were analyzed. Confocal pictures: *scale bar* 10 μm

in biopsies from both patients with *DNM2* mutations in which the characteristic transverse organization of the triads was largely lost in favor of a longitudinal distribution (Fig. 5). We also noted aberrant accumulation of SERCA1, a marker of the sarcoplasmic reticulum, between centralized nuclei in BIN1-mutated biopsies (Supplementary Fig. 3). In contrast, localization of alpha actinin (Z-line marker) appeared unaltered in all CNM biopsies, suggesting that disorganization of triads does not reflect a general defect in intracellular organization of muscle fibers (Figs. 5, 6). We conclude that, as for BIN1 localization, T-tubules and triads are consistently disorganized in the different forms of CNM.

Discussion

BIN1 is a ubiquitous membrane-tubulating protein mutated in autosomal cases of centronuclear myopathy. To understand the tissue-specific function of this protein and characterize the pathological mechanisms leading to the related diseases, we analyzed the only mouse model available for CNM and muscle biopsies from patients with the three different CNM forms and confirmed mutations in *BIN1*, *MTM1*, or *DNM2* genes. In the present study, we show that the PI-binding domain of BIN1 is present in all skeletal muscle isoforms in human and mice and is specifically associated with BIN1 localization at the triads in this tissue. We also highlighted BIN1 and triad defects as common hallmarks for all three forms of centronuclear myopathies.

Role and specificity of BIN1 in skeletal muscle

To gain insight into *BIN1* isoforms in skeletal muscle, we cloned and sequenced *BIN1* cDNAs from different tissues. The two RNA isoforms found in human and mouse skeletal muscles encompassed exon 11 encoding the PI-binding domain. Up to five isoforms were detected at the protein level [31], suggesting additional post-translational modification. It remains to be determined whether protein phosphorylation or other protein modifications, in addition to alternative splicing (inclusion of exon 11), is a main regulatory mechanism of BIN1 function in skeletal muscle. Butler et al. reported localization of BIN1 at T-tubules using a pan-isoform antibody [7]. Using an antibody directed against the PI-binding domain, we confirmed that BIN1 localizes close to the DHPR–RYR1 complex and the junction between the T-tubule and terminal cisternae of the sarcoplasmic reticulum, and showed that it is a marker of triad maturation around birth, evolving from a longitudinal to a transverse orientation (Figs. 3, 4, 5, 6). BIN1, DHPR, and RYR1 have been suggested to play a role in T-tubule/triad biogenesis in skeletal muscle [15, 24]. However, forced overexpression of the BIN1 SH3 domain in mouse led to sarcomere assembly defects and normal T-tubule biogenesis [14]. Together with our present findings, it suggests that the SH3 domain of BIN1 is involved in sarcomere integrity while the PI-binding domain drives the tubulation of membranes that form the triad in adult skeletal muscle.

Skeletal and cardiac muscles differ in the organization of the excitation–contraction coupling machinery as DHPR and RYR are in direct interaction and arranged into arrays of tetrads in skeletal muscle, while this is not the case in cardiac muscle [13]. Interestingly, the PI-binding domain of BIN1 is not present in cardiac muscle isoforms, suggesting that this domain is necessary for the specific formation of T-tubule/triad in skeletal muscle. Studies in mouse showed that BIN1 plays an important role in cardiac muscle development, as the *Bin1* knockout mouse died perinatally and displayed severe ventricular cardiomyopathy, while no striking histological abnormalities were reported in skeletal muscle [28]. However, CNM patients with *BIN1* mutations, patients with other CNM forms, and *Mtm1* KO mice do not present consistent cardiac involvement while skeletal muscles are defective, with alterations in T-tubule/triad organization (this study; [1, 6, 11, 20]). We hypothesize that, while total loss of *Bin1* in mouse perturbs heart development, *BIN1* mutations in CNM cause partial loss of function impacting specifically on skeletal muscle. Tissue-specific deletion of *Bin1* or specific deletion of the PI-binding domain will be required to challenge this hypothesis.

Common pathological mechanism in centronuclear myopathies

A recent review of the histopathology in several CNM patients pointed to differences within the established CNM forms and genetically unresolved cases [40]. The ARCNM biopsies we analyzed here (three different *BIN1* mutations) shared common features of CNM as centralization of nuclei and fiber atrophy. A very high percentage of central nuclei and accumulation of fat were most prominent in BIN1-mutated muscle biopsies. Specific alterations, such as invaginations of the sarcolemma and aberrant presence of vesicle-like structures, will have to be confirmed on additional patients before they may be used as diagnostic criteria.

Defects in triad organization have been recently noted in *mtm1* zebrafish morphants and in an *Mtm1* knockout mouse model, with dilated T-tubules and SR cisternae in zebrafish and longitudinal T-tubules in mouse [1, 11]. In this study we showed that, in addition to DHPR and RYR1, BIN1 localization was also disorganized in *Mtm1* KO mice. In

these mice, BIN1 and T-tubule defects preceded the appearance of muscle weakness. Similar BIN1 and T-tubule/triad defects appear as common features of the different CNM forms due to mutations in *MTM1*, *BIN1*, or *DNM2* in humans, suggesting that these proteins functionally interact. In agreement, Dowling et al. [11] recently showed that DHPR and RYR1 labeling was aberrant in three XLMTM patients. In both *mtm1* zebrafish morphants and in our present study on CNM patients, electron microscopy showed some defects in the triad structure. BIN1 accumulations around or between centralized nuclei were observed in patients with *BIN1* and *MTM1* mutations (Figs. 5, 6). Surprisingly, triad and BIN1 defects were marked in *DNM2*-mutated patients' biopsies, where DHPR, RYR1, and BIN1 were all distributed in a longitudinal orientation in contrast to their typical transverse pattern in normal skeletal muscle. As *DNM2*-mutated patients studied here are adults, these defects may have accumulated with time, suggesting the implication of DNM2 in the maintenance of triad organization.

Taken together, our findings suggest that the three forms of CNM share a common pathogenetic mechanism where BIN1 may represent a molecular link between myotubularin and dynamin 2 in skeletal muscle. *MTM1* encodes a PI phosphatase, and the skeletal muscle-specific exon of *BIN1* encodes a PI-binding domain. Moreover, BIN1 and DNM2 are well-known interactors in cultured cells although this molecular link remains to be explored in skeletal muscle. We hypothesize that MTM1 regulates the level and localization of specific PIs that either bind to BIN1 or serve as substrates to produce the PI that specifically binds BIN1. Amphiphysins have been shown to bind preferentially to PtdIns(4,5)P_2 rather than substrates and product of myotubularin activity (PtdIns3*P*, PtdIns(3,5)P_2, and PtdIns5*P*) [5, 21, 24, 43, 46]. Once membranes are remodeled by the action of BIN1, DNM2 may direct the adequate organization of the triads and/or their maintenance through cytoskeleton regulation. Indeed, DNM2 is a microtubule-binding protein which also plays a role in actin cytoskeleton assembly [42, 48]. An alternative hypothesis is the participation of BIN1 for the delivery of DHPR ion channels to the T-tubules as suggested recently by Hong et al. [17] based on their results in cardiac myocytes. Whether this mechanism is present in skeletal muscle remains to be determined.

In conclusion, BIN1 skeletal muscle isoforms appear to play an important role in triad formation, and this function is altered in several forms of centronuclear myopathies, where BIN1 and triad organization defects define a common pathogenetic mechanism. Molecular dissection of the roles of BIN1, myotubularin, and dynamin 2 in skeletal muscle will be required to understand the precise regulation of this pathway. Specifically, it will be important to elucidate what other functions BIN1 has in addition to its known role as a tumor suppressor.

Acknowledgments We thank Christine Kretz and the IGBMC imaging center for technical assistance. This work was supported by grants from Institut National de la Santé et de la Recherche Médicale (INSERM), Centre National de la Recherche Scientifique (CNRS), University of Strasbourg, Collège de France, Association Française contre les Myopathies (AFM), Fondation Recherche Médicale (FRM DEQ20071210538), Agence Nationale de la Recherche (ANR-06-MRAR 023, ANR-07-BLAN-0065-03, ANR-08-GENOPAT-005), and the E-rare program.

References

1. Al-Qusairi L, Weiss N, Toussaint A et al (2009) T-tubule disorganization and defective excitation-contraction coupling in muscle fibers lacking myotubularin lipid phosphatase. Proc Natl Acad Sci USA 106:18763–18768
2. Bevilacqua JA, Bitoun M, Biancalana V et al (2009) "Necklace" fibers, a new histological marker of late-onset MTM1-related centronuclear myopathy. Acta Neuropathol 117:283–291
3. Bitoun M, Bevilacqua JA, Prudhon B et al (2007) Dynamin 2 mutations cause sporadic centronuclear myopathy with neonatal onset. Ann Neurol 62:666–670
4. Bitoun M, Maugenre S, Jeannet PY et al (2005) Mutations in dynamin 2 cause dominant centronuclear myopathy. Nat Genet 37:1207–1209
5. Blondeau F, Laporte J, Bodin S, Superti-Furga G, Payrastre B, Mandel JL (2000) Myotubularin, a phosphatase deficient in myotubular myopathy, acts on phosphatidylinositol 3-kinase and phosphatidylinositol 3-phosphate pathway. Hum Mol Genet 9:2223–2229
6. Buj-Bello A, Laugel V, Messaddeq N et al (2002) The lipid phosphatase myotubularin is essential for skeletal muscle maintenance but not for myogenesis in mice. Proc Natl Acad Sci USA 99:15060–15065
7. Butler MH, David C, Ochoa GC et al (1997) Amphiphysin II (SH3P9; BIN1), a member of the amphiphysin/Rvs family, is concentrated in the cortical cytomatrix of axon initial segments and nodes of Ranvier in brain and around T tubules in skeletal muscle. J Cell Biol 137:1355–1367
8. Carson FL (1997) Histotechnology. ASCP press, Chicago
9. Claeys KG, Maisonobe T, Bohm J et al (2010) Phenotype of a patient with recessive centronuclear myopathy and a novel BIN1 mutation. Neurology 74:519–521
10. Denic V, Weissman JS (2007) A molecular caliper mechanism for determining very long-chain fatty acid length. Cell 130:663–677
11. Dowling JJ, Vreede AP, Low SE et al (2009) Loss of myotubularin function results in T-tubule disorganization in zebrafish and human myotubular myopathy. PLoS Genet 5:e1000372
12. Elliott K, Sakamuro D, Basu A et al (1999) Bin1 functionally interacts with Myc and inhibits cell proliferation via multiple mechanisms. Oncogene 18:3564–3573
13. Engel AG, Franzini-Armstrong C (2004) Myology, basic and clinical. McGraw-Hill, New York
14. Fernando P, Sandoz JS, Ding W et al (2009) Bin1 SRC homology 3 domain acts as a scaffold for myofiber sarcomere assembly. J Biol Chem 284:27674–27686
15. Flucher BE, Andrews SB, Daniels MP (1994) Molecular organization of transverse tubule/sarcoplasmic reticulum junctions during development of excitation-contraction coupling in skeletal muscle. Mol Biol Cell 5:1105–1118

16. Frost A, Unger VM, De Camilli P (2009) The BAR domain superfamily: membrane-molding macromolecules. Cell 137:191–196
17. Hong TT, Smyth JW, Gao D et al (2010) BIN1 localizes the L-type calcium channel to cardiac T-tubules. PLoS Biol 8:e1000312
18. Jeannet PY, Bassez G, Eymard B et al (2004) Clinical and histologic findings in autosomal centronuclear myopathy. Neurology 62:1484–1490
19. Johnson MA, Polgar J, Weightman D, Appleton D (1973) Data on the distribution of fibre types in thirty-six human muscles. An autopsy study. J Neurol Sci 18:111–129
20. Jungbluth H, Wallgren-Pettersson C, Laporte J (2008) Centronuclear (myotubular) myopathy. Orphanet J Rare Dis 3:26
21. Kojima C, Hashimoto A, Yabuta I et al (2004) Regulation of Bin1 SH3 domain binding by phosphoinositides. EMBO J 23:4413–4422
22. Laporte J, Biancalana V, Tanner SM et al (2000) MTM1 mutations in X-linked myotubular myopathy. Hum Mutat 15:393–409
23. Laporte J, Hu LJ, Kretz C et al (1996) A gene mutated in X-linked myotubular myopathy defines a new putative tyrosine phosphatase family conserved in yeast. Nat Genet 13:175–182
24. Lee E, Marcucci M, Daniell L et al (2002) Amphiphysin 2 (Bin1) and T-tubule biogenesis in muscle. Science 297:1193–1196
25. Leprince C, Romero F, Cussac D et al (1997) A new member of the amphiphysin family connecting endocytosis and signal transduction pathways. J Biol Chem 272:15101–15105
26. Luna LG (1992) Histopathological methods and color atlas of special stains and tissue artifacts. Johnson Printers, Downers Grove
27. McMahon HT, Gallop JL (2005) Membrane curvature and mechanisms of dynamic cell membrane remodelling. Nature 438:590–596
28. Muller AJ, Baker JF, DuHadaway JB et al (2003) Targeted disruption of the murine Bin1/Amphiphysin II gene does not disable endocytosis but results in embryonic cardiomyopathy with aberrant myofibril formation. Mol Cell Biol 23:4295–4306
29. Muller AJ, DuHadaway JB, Donover PS, Sutanto-Ward E, Prendergast GC (2004) Targeted deletion of the suppressor gene bin1/amphiphysin2 accentuates the neoplastic character of transformed mouse fibroblasts. Cancer Biol Ther 3:1236–1242
30. Nicot AS, Laporte J (2008) Endosomal phosphoinositides and human diseases. Traffic 9:1240–1249
31. Nicot AS, Toussaint A, Tosch V et al (2007) Mutations in amphiphysin 2 (BIN1) disrupt interaction with dynamin 2 and cause autosomal recessive centronuclear myopathy. Nat Genet 39:1134–1139
32. North K (2008) What's new in congenital myopathies? Neuromuscul Disord 18:433–442
33. Pelé M, Tiret L, Kessler JL, Blot S, Panthier JJ (2005) SINE exonic insertion in the PTPLA gene leads to multiple splicing defects and segregates with the autosomal recessive centronuclear myopathy in dogs. Hum Mol Genet 14:1417–1427
34. Pierson CR, Tomczak K, Agrawal P, Moghadaszadeh B, Beggs AH (2005) X-linked myotubular and centronuclear myopathies. J Neuropathol Exp Neurol 64:555–564
35. Prendergast GCMAJ, Ramalingam A, Chang MY (2009) Bar the door: cancer suppression by amphiphysin-like genes. Biochem Biophys Acta 1795:25–36
36. Ramjaun AR, McPherson PS (1998) Multiple amphiphysin II splice variants display differential clathrin binding: identification of two distinct clathrin-binding sites. J Neurochem 70:2369–2376
37. Razzaq A, Robinson IM, McMahon HT et al (2001) Amphiphysin is necessary for organization of the excitation-contraction coupling machinery of muscles, but not for synaptic vesicle endocytosis in Drosophila. Genes Dev 15:2967–2979
38. Ren G, Vajjhala P, Lee JS, Winsor B, Munn AL (2006) The BAR domain proteins: molding membranes in fission, fusion, and phagy. Microbiol Mol Biol Rev 70:37–120
39. Rezniczek GA, Konieczny P, Nikolic B et al (2007) Plectin 1f scaffolding at the sarcolemma of dystrophic (mdx) muscle fibers through multiple interactions with beta-dystroglycan. J Cell Biol 176:965–977
40. Romero NB (2010) Centronuclear myopathies: a widening concept. Neuromuscul Disord 20:223–228
41. Sakamuro D, Elliott KJ, Wechsler-Reya R, Prendergast GC (1996) BIN1 is a novel MYC-interacting protein with features of a tumour suppressor. Nat Genet 14:69–77
42. Shpetner HS, Vallee RB (1989) Identification of dynamin, a novel mechanochemical enzyme that mediates interactions between microtubules. Cell 59:421–432
43. Taylor GS, Maehama T, Dixon JE (2000) Inaugural article: myotubularin, a protein tyrosine phosphatase mutated in myotubular myopathy, dephosphorylates the lipid second messenger, phosphatidylinositol 3-phosphate. Proc Natl Acad Sci USA 97:8910–8915
44. Tiret L, Blot S, Kessler JL, Gaillot H, Breen M, Panthier JJ (2003) The cnm locus, a canine homologue of human autosomal forms of centronuclear myopathy, maps to chromosome 2. Hum Genet 113:297–306
45. Tosch V, Vasli N, Kretz C et al (2010) Novel molecular diagnostic approaches for X-linked centronuclear (myotubular) myopathy reveal intronic mutations. Neuromuscul Disord 20:375–381
46. Tronchere H, Laporte J, Pendaries C et al (2004) Production of phosphatidylinositol 5-phosphate by the phosphoinositide 3-phosphatase myotubularin in mammalian cells. J Biol Chem 279:7304–7312
47. Tsai TC, Horinouchi H, Noguchi S et al (2005) Characterization of MTM1 mutations in 31 Japanese families with myotubular myopathy, including a patient carrying 240 kb deletion in Xq28 without male hypogenitalism. Neuromuscul Disord 15:245–252
48. Unsworth KE, Mazurkiewicz P, Senf F et al (2007) Dynamin is required for F-actin assembly and pedestal formation by enteropathogenic *Escherichia coli* (EPEC). Cell Microbiol 9:438–449
49. Wechsler-Reya RJ, Elliott KJ, Prendergast GC (1998) A role for the putative tumor suppressor Bin1 in muscle cell differentiation. Mol Cell Biol 18:566–575

A Congenital Muscular Dystrophy with Mitochondrial Structural Abnormalities Caused by Defective De Novo Phosphatidylcholine Biosynthesis

Satomi Mitsuhashi,[1] Aya Ohkuma,[1] Beril Talim,[2] Minako Karahashi,[3] Tomoko Koumura,[3] Chieko Aoyama,[4] Mana Kurihara,[5] Ros Quinlivan,[6,7] Caroline Sewry,[6,8] Hiroaki Mitsuhashi,[1] Kanako Goto,[1] Burcu Koksal,[2] Gulsev Kale,[2] Kazutaka Ikeda,[9] Ryo Taguchi,[9] Satoru Noguchi,[1] Yukiko K. Hayashi,[1] Ikuya Nonaka,[1] Roger B. Sher,[10] Hiroyuki Sugimoto,[4] Yasuhito Nakagawa,[3] Gregory A. Cox,[10] Haluk Topaloglu,[11] and Ichizo Nishino[1,*]

Congenital muscular dystrophy is a heterogeneous group of inherited muscle diseases characterized clinically by muscle weakness and hypotonia in early infancy. A number of genes harboring causative mutations have been identified, but several cases of congenital muscular dystrophy remain molecularly unresolved. We examined 15 individuals with a congenital muscular dystrophy characterized by early-onset muscle wasting, mental retardation, and peculiar enlarged mitochondria that are prevalent toward the periphery of the fibers but are sparse in the center on muscle biopsy, and we have identified homozygous or compound heterozygous mutations in the gene encoding choline kinase beta (*CHKB*). This is the first enzymatic step in a biosynthetic pathway for phosphatidylcholine, the most abundant phospholipid in eukaryotes. In muscle of three affected individuals with nonsense mutations, choline kinase activities were undetectable, and phosphatidylcholine levels were decreased. We identified the human disease caused by disruption of a phospholipid de novo biosynthetic pathway, demonstrating the pivotal role of phosphatidylcholine in muscle and brain.

A spontaneous mutant mouse with a neonatal-onset autosomal-recessive rostral-to-caudal muscular dystrophy (*rmd* mouse) due to a loss-of-function mutation in choline kinase beta (*Chkb*) was identified in 2006.[1] Interestingly, *rmd* mice exhibit a unique mitochondrial morphology in muscle fibers, which show enlarged mitochondria at the periphery of the fiber but none at the center (Figure S1). These features are similar to those seen in a congenital muscular dystrophy (CMD) that we previously reported in four Japanese individuals.[2] We therefore screened 15 genetically undiagnosed cases of CMD with fairly homogenous clinical features (Table 1) for mutations in choline kinase beta (*CHKB*); we included the four cases from in our previous study in these 15 cases. Features included peculiar mitochondrial changes in muscle as well as motor delay followed by the appearance of severe mental retardation and microcephaly without structural brain abnormalities (Figure 1 and Table 1).

All clinical materials used in this study were obtained for diagnostic purposes with written informed consent. The study was approved by the Ethical Committee of the National Center of Neurology and Psychiatry. All mouse protocols were approved by the Ethical Review Committee on the Care and Use of Rodents in the National Institute of Neuroscience, National Center of Neurology and Psychiatry. For muscle pathology, samples of skeletal muscle were obtained from biceps brachii or quadriceps femoris in humans and from quadriceps femoris muscle in 8-week-old *rmd* mice. Muscles were frozen and sectioned at a thickness of 10 μm according to standard procedures, and a battery of routine histochemical stains, including hematoxylin and eosin (H&E), modified Gomori trichrome (mGT), NADH-tetrazolium reductase (NADH-TR), succinate dehydrogenase (SDH), cytochrome c oxidase (COX), and Oil Red O, were analyzed. For electron microscopic analysis, muscles were fixed as previously described,[3] and ultra-thin sections were observed at 120kV or 80kV. All affected individuals exhibited nonspecific dystrophic features (Figure 1A). However, in mGT, NADH-TR, SDH, and COX staining, prominent mitochondria at the periphery as well as central areas devoid of mitochondria were seen (Figures 1B and 1C). Oil Red O staining was unremarkable (data not shown). Electron microscopy confirmed enlarged mitochondria (Figure 1D).

We directly sequenced all exons and their flanking intronic regions in *CHKB* (MIM 612395, NM_005198.4, GenBank Gene ID 1120) in genomic DNA extracted from individuals' peripheral lymphocytes. All 15 individuals in three different populations (Japanese, Turkish, and British) had homozygous or compound heterozygous mutations in

[1]National Institute of Neuroscience, Department of Neuromuscular Research, National Center of Neurology and Psychiatry, Tokyo 1878502, Japan; [2]Department of Pediatrics, Pathology Unit, Hacettepe Children's Hospital, Ankara, 06100, Turkey; [3]School of Pharmaceutical Sciences, Kitasato University, Tokyo, 1088641, Japan; [4]Department of Biochemistry, Dokkyo Medical University School of Medicine, Mibu, 3210293, Japan; [5]Department of Pediatrics, The Kanagawa Rehabilitation Center, Kanagawa, 2430121, Japan; [6]Dubowitz Neuromuscular Centre, Great Ormond Street Hospital for Children NHS Trust, London, WC1N 3JH, UK; [7]MRC Centre for Neuromuscular Disorders, National Hospital for Neurology and Neurosurgery, Queen Square, London, WC1N 3BG, UK; [8]RJAH Orthopaedic Hospital, Oswestry, SY107AG, UK; [9]Department of Metabolome, Graduate School of Medicine, The University of Tokyo, Tokyo, 1130033, Japan; [10]The Jackson Laboratory, Bar Harbor, Maine, 04609, USA; [11]Department of Pediatrics, Child Neurology Unit, Hacettepe Children's Hospital, 06100, Ankara, Turkey
*Correspondence: nishino@ncnp.go.jp
DOI 10.1016/j.ajhg.2011.05.010.

Table 1. Summary of Clinical and Laboratory Features

			Phenotypic Findings									Muscle Pathology					Mutations				
Individual	Sex	Origin	Age at Last Follow-Up	Floppy at Birth	Walk Alone	Serum Creatine Kinase (IU/liter)	Head Circumference (percentile)	Mental Retardation	Seizure	Cardiomyopathy	Skin Change	Age at Muscle Biopsy	Necrotic Fiber	Regenerative Fiber	Endomysial Fibrosis	Mitochondrial Enlargement	Status	cDNA	Consequence	Exon	Literature ref. on phenotype
1	F	Japanese	died at 13 yr	+	2 yr 6 mo	370	ND	+	-	+	-	7 yr3 mo	+	+	+	+	homo	c.810T>A	p.Tyr270X	7	2
2	M	Japanese	died at 23 yr	+	1 yr 9 mo	190–2676	25–50	+	+	+	-	1 yr 2 mo	+	+	+	+	homo	c.810T>A	p.Tyr270X	7	2
3	F	Japanese	28 yr	+	1 yr 6 mo	502	ND	+	+	+	-	8 yr	+	+	+	+	het	c.116C>A	p.Ser39X	1	2
																	het	c.458dup	p.Leu153PhefsX57	3	2
4	M	Japanese	22 yr	+	2 yr 6 mo	230	3–10	+	+	-	-	4 yr 11 mo	+	+	+	+	het	c.116C>A	p.Ser39X	1	
																	het	c.458dup	p.Leu153PhefsX57	3	
5	M	Turkish	7 yr	-	2 yr 6 mo	843	<3	+	-	-	+	6 yr	±	+	+	+	homo	c.611_612insC	p.Thr205AsnfsX5	5	
6[a]	M	Turkish	died at 2 yr 6 mo	+	no	258	<3	+	-	+	-	1 yr 3 mo	±	±	+	+	homo	c.922C>T	p.Gln308X	8	
7	F	Turkish	2 yr	-	no	368	3-10	+	-	-[b]	-	9 mo	-	±	+	+	homo	c.847G>A	p.Glu283Lys	8	
8	M	Turkish	13 yr	ND	2 yr	1122	ND	+	-	-	-	12 yr 10 mo	±	±	+	+	homo	c.1130 G>T	p.Arg377Leu	11	
9	F	Turkish	17 yr	+	3 yr	2669	<3	+	-	ND	-	17 yr	±	±	+	+	homo	c.554_562del	p.Pro185_Trp187del	4	
10	F	Turkish	16 yr	+	3 yr	1103	<3	+	-	-[c]	+	3 yr	-	±	+	+	homo	c.677+1G>A	ND	5	
11	F	Turkish	3 yr 3 mo	+	no	497	10-25	+	-	ND	-	3 yr	±	-	+	+	homo	c.677+1G>A	ND	5	
12	F	Turkish	5 yr	-	3 yr 6 mo	467	25–50	+	-	-[d]	+	4 yr 6 mo	±	+	+	+	homo	c.677+1G>A	ND	5	
13	M	Turkish	3 yr 6 mo	+	no	428	<3	+	-	+	+	3 yr	+	+	+	+	homo	c.1031+1G>A	aberrant splicing	9	
14	F	Turkish	6 yr 4 mo	-	1 yr 3 mo	1606	3–10	+	-	+	-	4 yr	+	+	+	+	homo	c.1031+1G>A	ND	9	
15	M	British	died at 8 yr	-	3 yr 4 mo	607–1715	<3	+	-	+	+	2 yr 2 mo	+	-	+	+	homo	c.852_859del	p.Trp284X	8	

Detailed clinical information for individual 1 to 4 was previously described (2). Eleven CHKB mutations were identified in 15 affected individuals. All exhibited generalized muscle hypotonia and weakness from early infancy. Ambulation was delayed, and gait in those who achieved walking was limited. In addition, all displayed marked mental retardation, and most never acquired meaningful language. Microcephaly with head circumferences at or below the 3rd to 10th percentile was observed in most cases. Cranial magnetic resonance imaging showed no developmental brain defects. Six individuals had dilated cardiomyopathy, and two had cardiac anomaly. Individuals 1, 2, 6, and 15 died from cardiomyopathy at ages 13 yr, 23 yr, 2 yr 6 mo, and 8 yr, respectively. No one had respiratory insufficiency. Ichthyosiform skin changes were frequent. All showed mildly to moderately elevated serum creatine kinase (CK) levels. Individuals 7 and 9 also had homozygous single-nucleotide substitutions, c.902C>T (p.Thr301Ile) and c.983A>G (p.Gln328Arg), respectively. CHK activities of recombinant CHK-β proteins with p.Thr301Ile and p.Gln328Arg were only mildly decreased (Figure S2), suggesting these are likely to be neutral polymorphisms or only mildly hypomorphic mutations. Individuals 10, 11, and 12, who have same c.677+1G>A mutation, and individuals 13 and 14, who have same c.1031+1G>A mutation, are not siblings. Abbreviations are as follows: ND, not determined; p, percentile; F, female; and M, male.

[a] An affected sibling had ichthyosis and died at age 6 years with cardiomyopathy.
[b] Patent ductus arteriosus.
[c] Atrial septal defect.
[d] Mitral valve prolapse.

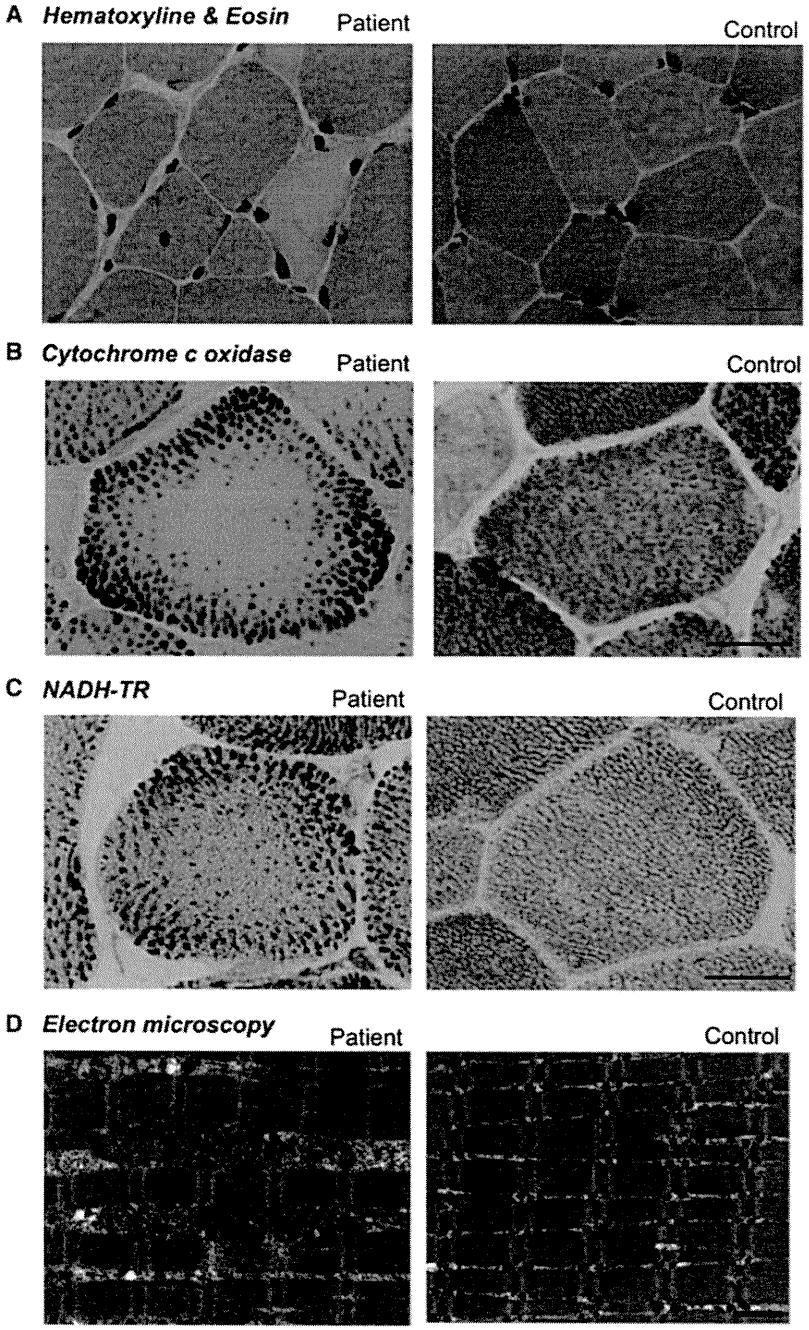

Figure 1. Muscle Pathology of the Affected Individuals

Cross-sections of muscle fiber from a human control and individual 4.

(A) On H&E staining, nonspecific dystrophic features with necrotic and regenerating fibers, internalized nuclei, and endomysial fibrosis are seen. The scale bar represents 25 μm.

(B) On cytochrome c oxidase staining, enlarged mitochondria at the periphery and central areas devoid of mitochondria were seen. The scale bar represents 20 μm.

(C) On NADH-TR staining, the intermyofibrillar network was preserved even in the central areas that are devoid of mitochondria, suggesting the presence of myofibrils and only absence of mitochondria. The scale bar represents 20 μm.

(D) Electron microscopy confirmed enlarged mitochondria. The scale bar represents 1 μm.

CHKB (Table 1). Among a total of 11 mutations identified, six were nonsense, two were missense, one was a 3 amino acid deletion, and two were splice-site mutations. The six nonsense mutations, c.116C>A (p.Ser39X), c.458dup (p.Leu153PhefsX57), c.611_612insC (p.Thr205AsnfsX5), c.810T>A (p.Tyr270X), c.852_859del (p.Trp284X), and c.922C>T (p.Gln308X), were predicted to truncate the protein and eliminate highly conserved domains of CHK.[4,5] Individuals 1 and 2 (unrelated, Japanese) had the same homozygous nonsense mutation of c.810T>A (p.Tyr270X). Individual 2's mother, who was healthy, had the heterozygous c.810T>A (p.Tyr270X) mutation. Unfortunately, a DNA sample from the father of individual 2 was not available. DNA samples from other family members of individual 1 and 2 were not available. Individuals 3 and 4 (siblings, Japanese) had the same compound heterozygous mutation c.116C>A (p.Ser39X) and c.458dup (p.Leu153PhefsX57). Both parents were healthy, and the father was heterozygous for mutation c.116C>A (p.Ser39X), whereas the mother was heterozygous for mutation c. 458dup (p.Leu153-PhefsX57), thus confirming a recessive inheritance pattern. These mutations cosegregated with the disease phenotype in all family members tested.

We therefore measured CHK activity in biopsied muscle. For all biochemical analyses, because of the limiting amounts of remaining tissue, biopsied muscle samples were available only from individuals 2, 3, and 4. Biopsied muscle samples from these three individuals were homogenized in 3 volumes of 20 mM Tris-HCl (pH 7.5), 154 mM KCl, and 1 mM phenylmethanesulfonyl fluoride with a sonicator (MISONIX), and supernatant fractions (105,000 × g, 60 min) were prepared and analyzed for CHK activity as previously described.[6] Similar to muscles of *rmd* mice,[1] muscles from individuals 2, 3, and 4, who carried homozygous or compound heterozygous nonsense mutations, did not have any detectable CHK activity (Figure 2A). Individuals 7, 8, and 9 had homozygous missense mutations c.847G>A (p.Glu283Lys) and c.1130 G>T (p.Arg377Leu) and a homozygous 3 amino acid deletion, c.554_562 del (p.Pro185_Trp187del), respectively.We screened 210 control chromosomes for the identified missense mutations and small in-frame deletion by direct sequencing or single-strand conformation polymorphism (SSCP) analysis. SSCP was performed with Gene Gel Excel (GE Healthcare) as previously described.[7] These missense mutations and this small in-frame deletion were not identified in control

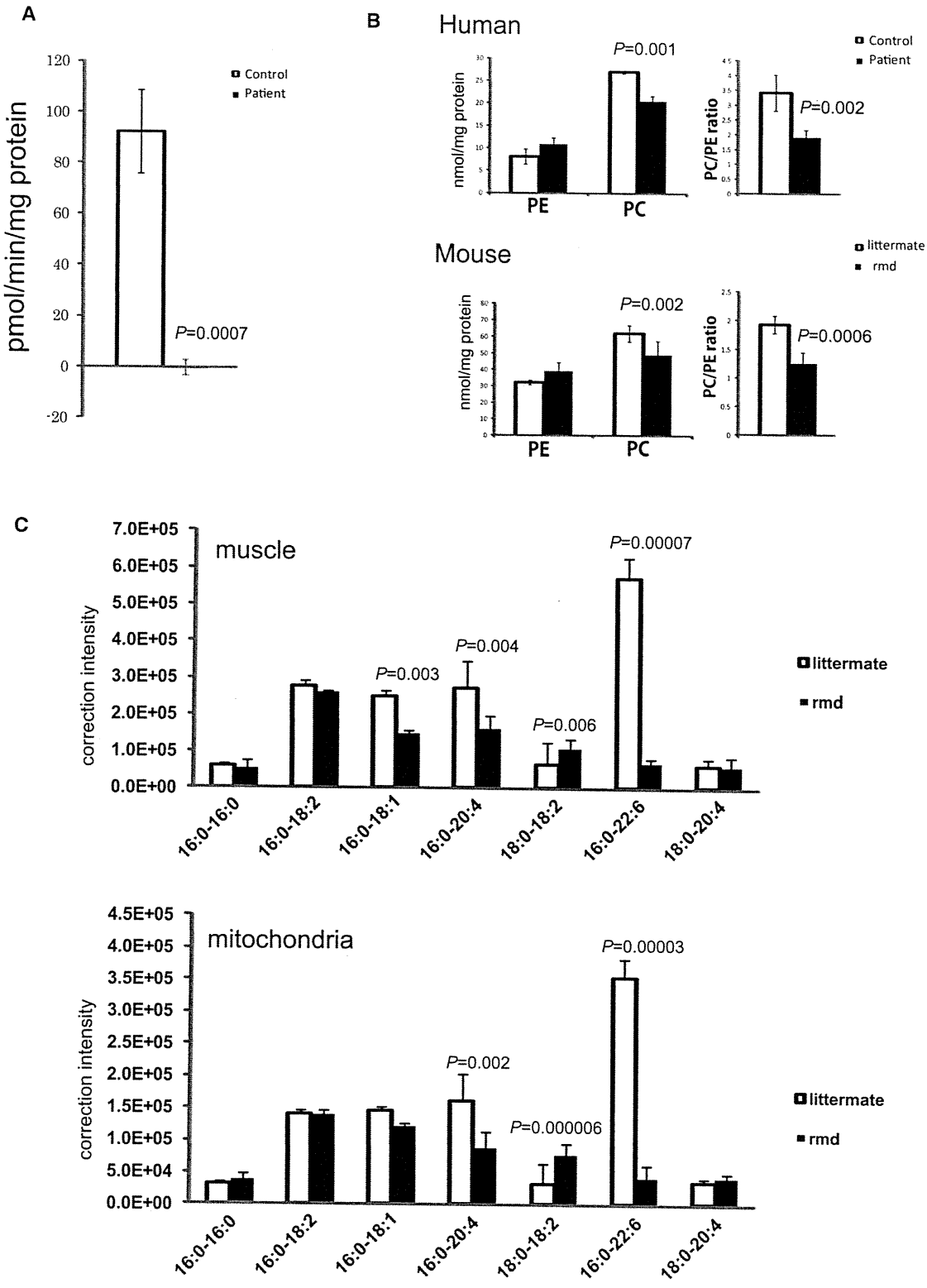

Figure 2. Choline Kinase Activity and Phospholipid Analyses
(A) In muscle tissue from individuals 2, 3, and 4, CHK activity cannot be detected (n = 3). Data represent the mean of three individuals. (B) PC and PE content in frozen biopsied muscle tissues from individuals 2, 3, and 4 and hindlimb muscles from 8-week-old *rmd* mice (n = 4) and control littermates (n = 5) were analyzed by thin-layer chromatography followed by phosphorus analysis. PC and the PC/PE ratio are significantly decreased in affected individuals and *rmd* mice (n = 3 for humans, n = 4 for *rmd* mice, n = 5 for littermates). (C) Fatty acid composition of PC molecular species in muscles and isolated mitochondria from hindlimb muscles of *rmd* mice are determined by electrospray ionization mass spectrometry (ESI-MS). We observed that 34:1-PC (16:0-18:1), 36:4-PC (16:0-20:4), and 38:6-PC (16:0-22:6) species are significantly decreased, whereas 36:2-PC (18:0-18:2) is increased in *rmd* muscle. Similarly, in isolated mitochondria from hindlimb muscle, 36:4-PC (16:0-20:4) and 38:6-PC (16:0-22:6) species are decreased, whereas 36:2-PC (18:0-18:2) is increased.

chromosomes. To elucidate the pathogenesis of these substitutions, we measured CHK activity in recombinant proteins with mutations. We cloned the open reading frame of *CHKB* into pGEM-T easy (Promega), then subcloned it into pET15b (Novagen) to make His-tagged CHK-β.[8] Each mutation was induced by site-directed mutagenesis.[7] Plasmids were transformed into *Escherichia coli* strain BL21 (DE3) and inoculated at 20°C to an OD_{600} of approximately 0.5, and the addition of 0.4 mM isopropyl-β-D-thiogalactopyranoside induced expression. The His-tagged CHK-β proteins were subjected to affinity purification on a nickel column (GE Healthcare) and eluted with 20 mM Tris-HCl (pH 7.4), 0.5 M NaCl, 300 mM imidazol, and 1 mM phenylmethanesulfonyl fluoride, and 25 ng protein was analyzed for CHK activity. CHK activity of recombinant proteins with these mutations decreased to less than 30% of wild-type CHK activity, suggesting that these mutations are causative in these individuals (Figure S2). For individual 13, who had a mutation at the splice site of the exon-intron border after exon 9 (c.1031+1G>A), we also analyzed cDNA sequences. Exons 4 through 10 were amplified from the first-strand cDNAs, and direct sequencing followed. cDNA analysis of *CHKB* in skeletal muscle from individual 13 showed four splicing variants, all of which remove consensus domains for *CHKB* (Figure S3). This suggests the same loss-of-function mechanism in humans and *rmd* mice.

Because phosphorylation of choline by CHK is the first enzymatic step for phosphatidylcholine (PC) biosynthesis,[9] we anticipated that PC content should be altered in affected individuals' muscles. Phosphatidylcholine (PC), phosphatidylethanolamine (PE), and total phospholipid amounts were measured in biopsied muscles from individuals 2, 3, and 4 and in leg muscles from 8-week-old *rmd* mice by either one-dimensional or two-dimensional thin-layer chromatography (TLC) followed by phosphorus analysis.[10,11] As expected, PC levels decreased in affected individuals' skeletal muscle (Figure 2B), as they did in *rmd* mice (Figure 2B and Sher et al.[1]), suggesting that the CMDs due to *CHKB* mutations in humans and *rmd* mice are not only pathologically but also pathomechanistically similar.

PC is present in all tissues and accounts for around 50% of phospholipids in biological membranes in eukaryotes. Selective tissue involvement can be explained by the different tissue distribution of CHK isoforms. There are two CHK isoforms: CHK-α and CHK-β, encoded by distinct genes, *CHKA* (MIM 118491) and *CHKB*, respectively. They are known to form both homodimers and heterodimers, with differential tissue distribution.[12] In mice, disruption of *Chka* causes embryonic lethality,[13] suggesting the importance of CHK-α in embryonic development. In skeletal muscles from *rmd* mice, CHK activity is absent, and PC levels are decreased.[1] In other tissues, however, CHK activity is only mildly decreased, PC levels are not altered, and no obvious pathological change is seen.[1] CHK activity in skeletal muscle from individuals 2, 3, and 4 is barely detectable, and PC levels are significantly decreased, suggesting that CHK-β is the major isoform in human skeletal muscle. In support of this notion, CHK-α was not detected in human muscle (Figure S4). These results suggest that muscular dystrophy in affected individuals and *rmd* mice is caused by a defect in muscle PC biosynthesis. In addition, in *rmd* mice, hindlimb muscles are more significantly affected than forelimb muscles.[1] This is most likely explained by the fact that CHK activity is detected, though decreased, in forelimb muscles in *rmd* mice as a result of the continued post-natal expression of *Chka*.[14] This indicates that the severity of muscle involvement is determined by the degree of deficiency of CHK activity.

Generally, phospholipids have saturated or monounsaturated fatty acids at the *sn-1* position and polyunsaturated fatty acids at the *sn-2* position of glycerol backbone.[15] It has been shown that phospholipids have tissue-specific fatty acid composition.[15] For example, heart PC and muscle PC mainly contain docosahexaenoic acid (22:6) (Nakanishi et al.[15] and Figure 2C), but liver PC includes various fatty acids.[15] NanoESI-MS analyses of PC molecular species in muscle and isolated mitochondria were performed with a 4000Q TRAP (AB SCIEX, Foster City, CA, USA) and a chip-based ionization source, TriVersa NanoMate (Advion BioSystems, Ithaca, NY, USA).[16] Quadriceps femoris (hindlimb) and Triceps (forelimb) muscle from affected *rmd* mice and littermate controls were frozen with liquid nitrogen, and total lipid was extracted by the Bligh and Dyer method.[10] The ion spray voltage was set at −1.25kV, gas pressure at 0.3 pound per square inch (psi), and flow rates at 200 nl/min. The scan range was set at m/z 400~1200, declustering potential at −100V, collision energies at −35~−45V, and resolutions at Q1 and Q3 "unit." The mobile phase composition was chloroform: methanol (1/2) containing 5 mM ammonium formate and was normalized to the muscle weight. The total lipids were directly subjected by flow injection, and selectivity was analyzed by neutral loss scanning of the polar head

In muscle and isolated mitochondria, the 38:6-PC molecular species is profoundly decreased (n = 6 for muscle, n = 5 for isolated mitochondria).

Mitochondria from skeletal muscles of whole hindlimbs of *rmd* mice were isolated by the differential centrifugation method. Fresh muscle was minced and homogenized with a motor-driven Teflon pestle homogenizer with ice-cold mitochondrial isolation buffer (10 mM Tris-HCl [pH 7.2], 320 mM sucrose, 1mM EDTA, 1mM DTT, 1 mM PMSF, 1 mg/ml BSA, and protease inhibitor cocktail [Roche]) and centrifuged at 1,500 × *g* for 5 min. The supernatant fraction was centrifuged at 15,000 × *g* for 20 min, the pellet was resuspended in mitochondrial isolation buffer, and the centrifugation/resuspension was repeated twice more.

All data are presented as means ± standard deviation (SD). Means were compared by analysis with a two-tailed t test via R software version 2.11.0.

group for PC in negative-ion mode.[17] Interestingly, there was a 10-fold decrease (9.8%) in the 16:0-22:6-PC levels versus the control in *rmd* hindlimb muscle and also in muscle mitochondria (Figure 2C), indicating the importance of the PC de novo synthesis pathway for maintaining not only PC levels but also fatty acid composition of PC molecular species. Similarly, in forelimb muscle 16:0-22:6 PC levels were also decreased in comparison to the control, but to a milder extent (18.2%), suggesting an association between severity of muscle damage and fatty acid composition alteration of PC (data not shown). In *rmd* mice, it has been shown that muscle PC can be delivered from plasma lipoprotein,[18] suggesting that non-decreased PC molecular species might be derived from the plasma, whereas 16:0-22:6 PC might be synthesized only in muscle (and possibly in brain). However, confirmation of this requires further studies.

Individuals with *CHKB* mutations have severe mental retardation in addition to the muscular dystrophy. Interestingly, polymorphisms near the *CHKB* locus and decreased CHKB expression have been associated with narcolepsy with cataplexy, suggesting a link between CHK-β activity and the maintenance of normal brain function in humans.[19] Furthermore, brain damage in pneumococcal infection has been attributed to the inhibition of de novo PC synthesis, suggesting the importance of PC synthesis for the brain.[20] Our data provide evidence that altered phospholipid biosynthesis is a causative agent for a human congenital muscular dystrophy, and further studies will elucidate the detailed molecular mechanisms of the disease in both muscle and brain.

Supplemental Data

Supplemental Data include four figures and can be found with this article online at http://www.cell.com/AJHG/.

Acknowledgments

We are grateful to the patients and their family for their participation, to Megumu Ogawa, Etsuko Keduka, Yuriko Kure, Mieko Ohnishi, Kaoru Tatezawa, and Kazu Iwasawa (National Center of Neurology and Psychiatry) for their technical assistance, to Naoki Kondou and Hiroyuki Taguchi (Kao Corporation) for their kind support on mass analysis, to Osamu Fujino and Kiyoshi Takahashi (Department of Pediatrics, Nippon Medical School) for providing patient information, and to Ken Inoue (National Center of Neurology and Psychiatry) for thoughtful comments on genetics. This study was supported partly by the Research on Psychiatric and Neurological Diseases and Mental Health of Health and Labour Sciences research grants; partly by Research on Intractable Diseases of Health and Labor Sciences research grants; partly by a Research Grant for Nervous and Mental Disorders (20B-12, 20B-13) from the Ministry of Health, Labour and Welfare; partly by an Intramural Research Grant (23-4, 23-5) for Neurological and Psychiatric Disorders from NCNP; partly by KAKENHI (20390250, 22791019); partly by Research on Publicly Essential Drugs and Medical Devices of Health and Labor Sciences research grants; partly by the Program for Promotion of Fundamental Studies in Health Sciences of the National Institute of Biomedical Innovation (NIBIO); and partly by a grant from the Japan Foundation for Neuroscience and Mental Health. G.A.C. and R.B S. were supported in part by a National Institutes of Health grant (AR-49043 to G.A.C.).

Received: March 21, 2011
Revised: April 21, 2011
Accepted: May 10, 2011
Published online: June 9, 2011

Web Resources

The URLs for data presented herein are as follows:

GenBank, http://www.ncbi.nlm.nih.gov/Genbank
Online Mendelian Inheritance in Man (OMIM), http://www.omim.org
R software version 2.11.0, http://www.r-project.org/

References

1. Sher, R.B., Aoyama, C., Huebsch, K.A., Ji, S., Kerner, J., Yang, Y., Frankel, W.N., Hoppel, C.L., Wood, P.A., Vance, D.E., and Cox, G.A. (2006). A rostrocaudal muscular dystrophy caused by a defect in choline kinase beta, the first enzyme in phosphatidylcholine biosynthesis. J. Biol. Chem. *281*, 4938–4948.
2. Nishino, I., Kobayashi, O., Goto, Y., Kurihara, M., Kumagai, K., Fujita, T., Hashimoto, K., Horai, S., and Nonaka, I. (1998). A new congenital muscular dystrophy with mitochondrial structural abnormalities. Muscle Nerve *21*, 40–47.
3. Hayashi, Y.K., Matsuda, C., Ogawa, M., Goto, K., Tominaga, K., Mitsuhashi, S., Park, Y.E., Nonaka, I., Hino-Fukuyo, N., Haginoya, K., et al. (2009). Human PTRF mutations cause secondary deficiency of caveolins resulting in muscular dystrophy with generalized lipodystrophy. J. Clin. Invest. *119*, 2623–2633.
4. Liao, H., Aoyama, C., Ishidate, K., and Teraoka, H. (2006). Deletion and alanine mutation analyses for the formation of active homo- or hetero-dimer complexes of mouse choline kinase-α and -β. Biochim. Biophys. Acta *1761*, 111–120.
5. Aoyama, C., Yamazaki, N., Terada, H., and Ishidate, K. (2000). Structure and characterization of the genes for murine choline/ethanolamine kinase isozymes alpha and beta. J. Lipid Res. *41*, 452–464.
6. Ishidate, K., and Nakazawa, Y. (1992). Choline/ethanolamine kinase from rat kidney. Methods Enzymol. *209*, 121–134.
7. Matsumoto, H., Hayashi, Y.K., Kim, D.S., Ogawa, M., Murakami, T., Noguchi, S., Nonaka, I., Nakazawa, T., Matsuo, T., Futagami, S., et al. (2005). Congenital muscular dystrophy with glycosylation defects of α-dystroglycan in Japan. Neuromuscul. Disord. *15*, 342–348.
8. Mitsuhashi, H., Futai, E., Sasagawa, N., Hayashi, Y., Nishino, I., and Ishiura, S. (2008). Csk-homologous kinase interacts with SHPS-1 and enhances neurite outgrowth of PC12 cells. J. Neurochem. *105*, 101–112.
9. Aoyama, C., Liao, H., and Ishidate, K. (2004). Structure and function of choline kinase isoforms in mammalian cells. Prog. Lipid Res. *43*, 266–281.
10. Bligh, E.G., and Dyer, W.J. (1959). A rapid method of total lipid extraction and purification. Can. J. Biochem. Physiol. *37*, 911–917.
11. Rouser, G., Fkeischer, S., and Yamamoto, A. (1970). Two dimensional then layer chromatographic separation of polar

lipids and determination of phospholipids by phosphorus analysis of spots. Lipids *5*, 494–496.

12. Aoyama, C., Ohtani, A., and Ishidate, K. (2002). Expression and characterization of the active molecular forms of choline/ethanolamine kinase-α and -β in mouse tissues, including carbon tetrachloride-induced liver. Biochem. J. *363*, 777–784.
13. Wu, G., Aoyama, C., Young, S.G., and Vance, D.E. (2008). Early embryonic lethality caused by disruption of the gene for choline kinase alpha, the first enzyme in phosphatidylcholine biosynthesis. J. Biol. Chem. *283*, 1456–1462.
14. Wu, G., Sher, R.B., Cox, G.A., and Vance, D.E. (2010). Differential expression of choline kinase isoforms in skeletal muscle explains the phenotypic variability in the rostrocaudal muscular dystrophy mouse. Biochim. Biophys. Acta *1801*, 446–454.
15. Nakanishi, H., Iida, Y., Shimizu, T., and Taguchi, R. (2010). Separation and quantification of sn-1 and sn-2 fatty acid positional isomers in phosphatidylcholine by RPLC-ESIMS/MS. J. Biochem. *147*, 245–256.
16. Ikeda, K., Mutoh, M., Teraoka, N., Nakanishi, H., Wakabayashi, K., and Taguchi, R. (2011). Increase of oxidant-related triglycerides and phosphatidylcholines in serum and small intestinal mucosa during development of intestinal polyp formation in Min mice. Cancer Sci. *102*, 79–87.
17. Taguchi, R., Houjou, T., Nakanishi, H., Yamazaki, T., Ishida, M., Imagawa, M., and Shimizu, T. (2005). Focused lipidomics by tandem mass spectrometry. J. Chromatogr. B Analyt. Technol. Biomed. Life Sci. *823*, 26–36.
18. Wu, G., Sher, R.B., Cox, G.A., and Vance, D.E. (2009). Understanding the muscular dystrophy caused by deletion of choline kinase beta in mice. Biochim. Biophys. Acta *1791*, 347–356.
19. Miyagawa, T., Kawashima, M., Nishida, N., Ohashi, J., Kimura, R., Fujimoto, A., Shimada, M., Morishita, S., Shigeta, T., Lin, L., et al. (2008). Variant between CPT1B and CHKB associated with susceptibility to narcolepsy. Nat. Genet. *40*, 1324–1328.
20. Zweigner, J., Jackowski, S., Smith, S.H., Van Der Merwe, M., Weber, J.R., and Tuomanen, E.I. (2004). Bacterial inhibition of phosphatidylcholine synthesis triggers apoptosis in the brain. J. Exp. Med. *200*, 99–106.